

Luminescent Complexes of Iridium(III) Containing N<sup>∧</sup>C<sup>∧</sup>N-Coordinating Terdentate LigandsAndrew J. Wilkinson,<sup>†</sup> Horst Puschmann,<sup>‡</sup> Judith A. K. Howard,<sup>‡</sup> Clive E. Foster,<sup>§</sup> and J. A. Gareth Williams<sup>\*†</sup>*Department of Chemistry, University of Durham, South Road, Durham, DH1 3LE U.K., and Fujifilm Imaging Colorants Ltd, P.O. Box 42, Hexagon House, Blackley, Manchester, M9 8ZS U.K.*

Received June 27, 2006

A family of bis-terdentate iridium(III) complexes is reported which contain a cyclometalated, N<sup>∧</sup>C<sup>∧</sup>N-coordinating 1,3-di(2-pyridyl)benzene derivative. This coordination mode is favored by blocking competitive cyclometalation at the C<sup>4</sup> and C<sup>6</sup> positions of the ligand. Thus, 1,3-di(2-pyridyl)-4,6-dimethylbenzene (dpyxH) reacts with IrCl<sub>3</sub>·3H<sub>2</sub>O to generate a dichlorobridged dimer [Ir(dpyx-N,C,M)Cl(μ-Cl)]<sub>2</sub>, **1**. This dimer is cleaved by DMSO to give [Ir(dpyx)-(DMSO)Cl<sub>2</sub>], the X-ray crystal structure of which is reported here, confirming the N<sup>∧</sup>C<sup>∧</sup>N coordination mode of dpyx. The dimer **1** can also be cleaved by a variety of other ligands to generate novel classes of mononuclear complexes. These include charge-neutral bis-terdentate complexes of the form [Ir(N<sup>∧</sup>C<sup>∧</sup>N)(C<sup>∧</sup>N<sup>∧</sup>C)] and [Ir(N<sup>∧</sup>C<sup>∧</sup>N)(C<sup>∧</sup>N<sup>∧</sup>O)], by reaction of **1** with C<sup>∧</sup>N<sup>∧</sup>C-coordinating ligands (e.g., 2,6-diphenylpyridine and derivatives) and C<sup>∧</sup>N<sup>∧</sup>O-coordinating ligands (based on 6-phenylpicolinate), respectively. Treatment of **1** with terpyridines leads to dicationic complexes of the type [Ir(N<sup>∧</sup>C<sup>∧</sup>N)(N<sup>∧</sup>N<sup>∧</sup>N)]<sup>2+</sup>, while 2-phenylpyridine gives [Ir(dpyx-N<sup>∧</sup>C<sup>∧</sup>M)-(ppy-C,M)Cl]. All of the charge-neutral complexes are luminescent in fluid solution at room temperature. Assignment of the emission to charge-transfer excited states with significant MLCT character is supported by DFT calculations. In the [Ir(N<sup>∧</sup>C<sup>∧</sup>N)(C<sup>∧</sup>N<sup>∧</sup>C)] class, fluorination of the C<sup>∧</sup>N<sup>∧</sup>C ligand at the phenyl 2' and 4' positions leads to a blue-shift in the emission and to an increase in the quantum yield ( $\lambda_{\text{max}} = 547 \text{ nm}$ ,  $\phi = 0.41$  in degassed CH<sub>3</sub>CN at 295 K) compared to the nonfluorinated parent complex ( $\lambda_{\text{max}} = 585 \text{ nm}$ ,  $\phi = 0.21$ ), as well as to a stabilization of the compound with respect to photodissociation through cleavage of mutually trans Ir–C bonds. [Ir(dpyx-N<sup>∧</sup>C<sup>∧</sup>M)(ppy-C,M)Cl] is an exceptionally bright emitter:  $\phi = 0.76$ ,  $\lambda_{\text{max}} = 508 \text{ nm}$ , in CH<sub>3</sub>CN at 295 K. In contrast, the [Ir(N<sup>∧</sup>C<sup>∧</sup>N)(C<sup>∧</sup>N<sup>∧</sup>O)] complexes are much less emissive, shown to be due to fast nonradiative decay of the excited state, probably involving reversible Ir–O bond cleavage. The [Ir(N<sup>∧</sup>C<sup>∧</sup>N)(N<sup>∧</sup>N<sup>∧</sup>N)]<sup>2+</sup> complexes are very feeble emitters even at 77 K, probably due to the almost exclusively interligand charge-transfer nature of the lowest-energy excited state in these complexes.

## Introduction

Interest in the photochemistry of second- and third-row transition metal complexes with polypyridyl ligands grew rapidly in the 1970s, as the potential of compounds such as [Ru(bpy)<sub>3</sub>]<sup>2+</sup> as excited-state electron-transfer agents emerged.<sup>1,2</sup> This interest has been maintained, indeed accelerated, by new applications such as light-emitting devices

and luminescent probes and sensors.<sup>3,4</sup> For many years, iridium played the part of Cinderella alongside its three sisters Ru, Os, and Pt, probably reflecting the kinetic inertness of the Ir(III) ion: harsh conditions and laborious purification

\* To whom correspondence should be addressed. E-mail: j.a.g.williams@durham.ac.uk.

<sup>†</sup> Coordination Photochemistry Group, University of Durham.

<sup>‡</sup> Chemical Crystallography Group, University of Durham.

<sup>§</sup> Fujifilm Imaging Colorants Ltd.

- (1) Work in the field from the 1970s and 1980s has been extensively reviewed; see for example Balzani, V.; Scandola, F. *Supramolecular Photochemistry*; Ellis Horwood: New York, 1991.
- (2) Hoffman, M. Z., Ed. *Inorganic Photochemistry: State of the Art. J. Chem. Educ.* **1983**, *60*, 784–887.
- (3) For a review of the science of OLEDs, see, for example: Hung, L. S.; Chen, C. H. *Mater. Sci. Eng. Rep.* **2002**, *39*, 143.
- (4) Schanze, K. S.; Schmehl, R. H., Eds. *Applications of Inorganic Photochemistry in the Chemical and Biological Sciences—Contemporary Developments. J. Chem. Educ.* **1997**, *74*, 633–702.

are often required for the formation of its complexes, the synthesis of  $[\text{Ir}(\text{bpy})_3]^{3+}$  being a good example.<sup>5</sup> Thus, notwithstanding some pioneering work in the 1980s, particularly by Watts and co-workers,<sup>6</sup> it is principally in the past decade that the photophysics and photochemistry of iridium complexes have begun to enjoy widespread investigation.<sup>7</sup>

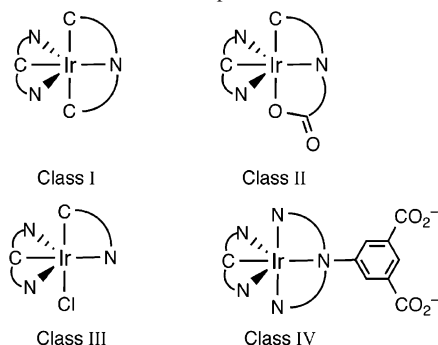
$\text{N}_6$ -coordinated iridium complexes {e.g.  $[\text{Ir}(\text{bpy})_3]^{3+}$ ,  $[\text{Ir}(\text{tpy})_2]^{3+}$ , and their derivatives} are typically characterized by long-lived emissive excited states of primarily  $^3\pi-\pi^*$  character<sup>5,8,9</sup> or, when strongly electron-donating substituents are present in the ligands, intraligand charge transfer states (ILCT).<sup>10,11</sup> This contrasts with the unambiguous metal-to-ligand charge transfer (MLCT) nature of Ru(II) analogues<sup>12</sup> and arises from the higher oxidation state of the iridium metal center (+3 rather than +2): this raises the energy of the MLCT transitions in such Ir(III) complexes, normally to beyond those of the intraligand excited states of the pyridyl ligands. On the other hand, the introduction of anionic ligands into the coordination sphere of the iridium ion (e.g., chloride or a cyclometalating carbon) stabilizes the MLCT excited states and/or elicits the possibility of interligand charge-transfer transitions.<sup>7</sup>

Tris-cyclometalated complexes such as *fac*- $[\text{Ir}(\text{ppy})_3]$  have attracted particular attention in the field of organic light-emitting devices (OLEDs).<sup>13–15</sup> The high efficiency of their emission from triplet MLCT states, together with their good chemical and photochemical stability and their charge neutrality, offers potential as dopants for harvesting the otherwise nonemissive triplet states formed in such devices.

The large increases in device efficiency shown to be possible have provided a major impetus for the recent synthesis and investigation of a large range of derivatives of the  $\text{Ir}(\text{N}\wedge\text{C})_3$ ,  $\text{Ir}(\text{N}\wedge\text{C})_2(\text{L}\wedge\text{X})$ , and  $\text{Ir}(\text{N}\wedge\text{N}^-)_3$  structural classes  $\{\text{N}\wedge\text{C} = \text{bidentate cyclometalating ligands such as ppy; L}\wedge\text{X} = \text{anionic ligands such as acac and 2-picolate; N}\wedge\text{N}^- = 5\text{-(2-pyridyl)pyrazoles and 5-(2-pyridyl)triazoles}\}$ .<sup>16–18</sup> In parallel, bis-cyclometalated iridium complexes, particularly those of the form  $[\text{Ir}(\text{N}\wedge\text{C})_2(\text{N}\wedge\text{N})]^+$  ( $\text{N}\wedge\text{N} = \text{bipyridine ligands}$ ), have been studied as sensitizers for energy- and electron-transfer reactions, for which they are particularly appropriate given the long-lived nature of their excited states, the tunability of the excited-state energies, and their strong photoreducing properties.<sup>19</sup> Applications in luminescent probe and sensor molecules are also under investigation.<sup>20</sup>

Almost all such work on cyclometalated iridium complexes has focused hitherto on tris-bidentate complexes, primarily of the generic types indicated above. In contrast, cyclometalated iridium complexes containing two *terdentate* ligands have seen little investigation, despite the widely recognized structural advantages of bis-terdentate complexes over tris-bidentate analogues.<sup>21</sup> For example, the latter are normally chiral, so that a mixture of diastereomers is formed when two or more such complexes are linked together, whereas the former are achiral. Also, the axial symmetry of complexes with two terdentate ligands allows three or more such complexes to be connected linearly and without problems of geometrical isomerism. Scandola and co-workers recently described a series of cationic  $[\text{Ir}(\text{N}\wedge\text{N}\wedge\text{N})(\text{C}\wedge\text{N}\wedge\text{C})]^+$  complexes<sup>22</sup> ( $\text{N}\wedge\text{N}\wedge\text{N} = \text{terpyridyl ligand}$ ;  $\text{C}\wedge\text{N}\wedge\text{C} = 2,6\text{-diphenylpyridyl ligand}$ ), while Mamo and colleagues earlier

- (5) Flynn, C. M., Jr.; Demas, J. N. *J. Am. Chem. Soc.* **1974**, *96*, 1959.  
 (6) (a) Sprouse, S.; King, K. A.; Spellane, P. J.; Watts, R. J. *J. Am. Chem. Soc.* **1984**, *106*, 6647. (b) King, K. A.; Watts, R. J. *J. Am. Chem. Soc.* **1987**, *109*, 1589. (c) Garces, F. O.; King, K. A.; Watts, R. J. *Inorg. Chem.* **1988**, *27*, 3464.  
 (7) A concise review at the beginning of the millenium was provided by: Dixon, I. M.; Collin, J.-P.; Sauvage, J.-P.; Flamigni, L.; Encinas, S.; Barigelletti, F. *Chem. Soc. Rev.* **2000**, *29*, 385.  
 (8) (a) Ayala, N. P.; Flynn, C. M., Jr.; Sacksteder, L.; Demas, J. N.; DeGraff, B. A. *J. Am. Chem. Soc.* **1990**, *112*, 3837. (b) Collin, J.-P.; Dixon, I. M.; Sauvage, J.-P.; Williams, J. A. G.; Barigelletti, F.; Flamigni, L. *J. Am. Chem. Soc.* **1999**, *121*, 1493.  
 (9) (a) Licini, M.; Williams, J. A. G. *Chem. Commun.* **1999**, 1943. (b) Goodall, W.; Williams, J. A. G. *J. Chem. Soc., Dalton Trans.* **2000**, 2893. (c) Leslie, W.; Batsanov, A. S.; Howard, J. A. K.; Williams, J. A. G. *Dalton Trans.* **2004**, 623. (d) Arm, K. J.; Leslie, W.; Williams, J. A. G. *Inorg. Chim. Acta* **2006**, *359*, 1222. (e) Bexon, A. J. S.; Williams, J. A. G. *C. R. Chim.* **2005**, *8*, 1326.  
 (10) Leslie, W.; Poole, R. A.; Murray, P. R.; Yellowlees, L. J.; Beeby, A.; Williams, J. A. G. *Polyhedron* **2004**, *23*, 2769.  
 (11) Note, however, that the proportion of MLCT character in the excited state increases upon introduction of electron-withdrawing groups into the ligands: (a) Baranoff, E.; Dixon, I. M.; Collin, J.-P.; Sauvage, J.-P.; Ventura, B.; Flamigni, L. *Inorg. Chem.* **2004**, *43*, 3057. (b) Flamigni, L.; Ventura, B.; Barigelletti, F.; Baranoff, E.; Collin, J.-P.; Sauvage, J.-P. *Eur. J. Inorg. Chem.* **2005**, 1312.  
 (12) Watts, R. J. *J. Chem. Educ.* **1983**, *60*, 834.  
 (13) (a) Baldo, M. A.; Lamansky, S.; Burrows, P. E.; Thompson, M. E.; Forrest, S. R. *Appl. Phys. Lett.* **1999**, *75*, 4. (b) Baldo, M. A.; Thompson, M. E.; Forrest, S. R. *Pure Appl. Chem.* **1999**, *71*, 2095. (c) Adachi, C.; Baldo, M. A.; Forrest, S. R.; Thompson, M. E. *Appl. Phys. Lett.* **2000**, *77*, 904. (d) Adachi, C.; Baldo, M. A.; Thompson, M. E.; Forrest, S. R. *J. Appl. Phys.* **2001**, *90*, 5048.  
 (14) Grushin, V. V.; Herron, N.; LeCloux, D. D.; Marshall, W. J.; Petrov, V. A.; Wang, Y. *Chem. Commun.* **2001**, 1494.  
 (15) (a) Tsuzuki, T.; Shirasawa, N.; Suzuki, T.; Tokito, S. *Adv. Mater.* **2003**, *15*, 1455. (b) Laskar, L. R.; Chen, T.-M. *Chem. Mater.* **2004**, *16*, 111.  
 (16) (a) Lamansky, S.; Djurovich, P. I.; Abdel-Razzaq, F.; Lee, H.; Adachi, C.; Burrows, P. E.; Forrest, S. R.; Thompson, M. E. *J. Am. Chem. Soc.* **2001**, *123*, 4304. (b) Lamansky, S.; Djurovich, P. I.; Murphy, D.; Abdel-Razzaq, F.; Kwong, R.; Tsyba, I.; Bortz, M.; Mui, B.; Bau, R.; Thompson, M. E. *Inorg. Chem.* **2001**, *40*, 1704.  
 (17) Schaffner-Hamann, C.; von Zelewsky, A.; Barbieri, A.; Barigelletti, F.; Muller, G.; Riehl, J. P.; Neels, A. *J. Am. Chem. Soc.* **2004**, *126*, 9339.  
 (18) (a) Su, Y.-J.; Juang, H.-L.; Li, C.-L.; Chien, C.-H.; Tao, Y.-T.; Chou, P.-T.; Datta, S.; Liu, R. S. *Adv. Mater.* **2003**, *15*, 884. (b) Yang, C.-H.; Tai, C.-C.; Sun, I.-W. *J. Mater. Chem.* **2004**, *14*, 947. (c) Duan, J.-P.; Sun, P.-P.; Cheng, C.-H. *Adv. Mater.* **2003**, *15*, 224. (d) Huang, W.-S.; Lin, J. T.; Chien, C.-H.; Tao, Y.-T.; Sun, S.-S.; Wen, Y.-S. *Chem. Mater.* **2004**, *16*, 2480. (e) Coppo, P.; Plummer, E. A.; De Cola, L. *Chem. Commun.* **2004**, 1774.  
 (19) (a) Ortmans, I.; Didier, P.; Kirsch-De Mesmaecker, A. *Inorg. Chem.* **1995**, *35*, 3695. (b) van Diemen, J. H.; Hage, R.; Haasnoot, J. G.; Lempers, H. E. B.; Reedijk, J.; Vos, J. G.; De Cola, L.; Barigelletti, F.; Balzani, V. *Inorg. Chem.* **1992**, *31*, 3518. (c) Serroni, S.; Juris, A.; Campagna, S.; Venturi, M.; Denti, G.; Balzani, V. *J. Am. Chem. Soc.* **1994**, *116*, 9086. (d) Arm, K. J.; Williams, J. A. G. *Chem. Commun.* **2005**, 232. (e) Sabatini, C.; Barbieri, A.; Barigelletti, F.; Arm, K. J.; Williams, J. A. G. *Photochem. Photobiol. Sci.* **2006**, in press. (f) Welter, S.; Lafolet, F.; Cecchetto, E.; Vergeer, F.; De Cola, L. *ChemPhysChem* **2005**, *6*, 2417.  
 (20) For example, Lo et al. have pioneered investigations into biotin-appended  $[\text{Ir}(\text{N}\wedge\text{C})_2(\text{N}\wedge\text{N})]^+$  complexes, the subject of a recent review: Lo, K. K. W.; Hui, W. K.; Chung, C. K.; Tsang, K. H. K.; Ng, D. C. M.; Zhu, N. Y.; Cheung, K. K. *Coord. Chem. Rev.* **2005**, *249*, 1434.  
 (21) A review of the concept is provided by: Sauvage, J.-P.; Collin, J.-P.; Chambron, J.-C.; Guillerez, S.; Coudret, C.; Balzani, V.; Barigelletti, F.; De Cola, L.; Flamigni, L. *Chem. Rev.* **1994**, *94*, 993.  
 (22) (a) Polson, M.; Fracasso, S.; Bertolasi, V.; Ravaglia, M.; Scandola, F. *Inorg. Chem.* **2004**, *43*, 1950. (b) Polson, M.; Ravaglia, M.; Fracasso, S.; Garavelli, M.; Scandola, F. *Inorg. Chem.* **2005**, *44*, 1282.

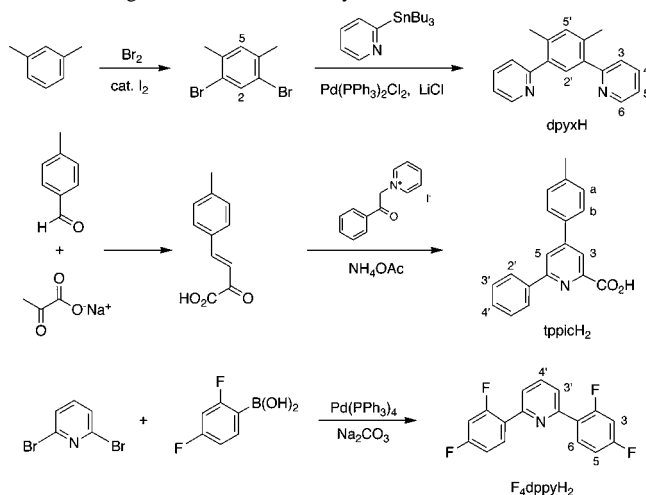
**Scheme 1.** Schematic Structures of the Four Proposed Classes of Charge-Neutral, Bis-terdentate Complexes of Iridium

isolated cationic complexes containing either one or two  $N\wedge C$ -coordinated 2,6-bis(2'-quinolyl)pyridine ligands.<sup>23</sup>

We embarked upon a program to investigate the complexation chemistry of iridium with terdentate, cyclometalating ligands and to explore their excited-state and luminescence properties. Aside from the structural advantages with respect to incorporation into multimetallic systems discussed above, improved stabilities could, in principle, be envisaged upon switching from bidentate to terdentate ligands, and new approaches to tuning excited state energies opened up. In particular, we sought to obtain charge-neutral complexes since these are generally preferred over charged compounds in applications such as OLEDs, the latter often suffering from poorer device lifetimes and long turn-on times due to the redistribution of ions under the applied electric field.<sup>24</sup>

## Results and Discussion

**1. Strategy.** Our strategy has been to use a 2,6-dipyridyl-benzene derivative as a formally monoanionic, cyclometalating ligand offering terdentate  $N\wedge C\wedge N$  coordination in combination with a second, dianionic terdentate ligand to generate an Ir(III) complex with overall charge neutrality (Scheme 1). Two distinct classes of dianionic ligand have been investigated in this study, namely bis-cyclometalating  $C\wedge N\wedge C$ -coordinating ligands such as 2,6-diphenylpyridine (Class I in Scheme 1) and  $C\wedge N\wedge O^-$  ligands based on 6-phenylpicolinate, where  $O^-$  is a carboxylate oxygen (Class II). We previously reported the first example of the first class in a communication in this journal.<sup>25</sup> Here, we describe in detail the synthetic chemistry and photophysical properties of the two classes, as well as a highly emissive complex incorporating the combination of 2-phenylpyridine ( $N\wedge C$ ) and chloride ( $X^-$ ) in place of the terdentate dianionic ligand (Class III). We also considered the principle of using an  $N\wedge N\wedge N$ -coordinating terpyridyl ligand carrying two ionisable carboxylic acid groups as an alternative type of dianionic ligand to furnish a charge-neutral complex (Class IV) for which purpose an investigation of the properties of model

**Scheme 2.** Synthetic Strategies Employed in the Preparation of the Terdentate Ligands Used in This Study<sup>a</sup>

<sup>a</sup> The numbering system used in the assignment of the <sup>1</sup>H NMR spectra of the uncoordinated ligands is included.

[Ir( $N\wedge C\wedge N$ )( $N\wedge N\wedge N$ )]<sup>2+</sup> complexes has been carried out. Haga et al. have also been investigating complexes related to those of Classes III and IV recently, but based on 1,3-bis-(1-methyl-benzimidazol-2-yl)benzene as the  $N\wedge C\wedge N$  ligand.<sup>26</sup>

**2. Synthesis of the Required Ligands. 2.1.  $N\wedge C\wedge N$  Ligands.** The palladium-catalyzed Stille cross-coupling of 1,3-dibromobenzenes with 2-(trialkylstannyl)-pyridines has previously been shown to offer a reliable route to 1,3-di(2-pyridyl)-benzene (dpybH) and derivatives,<sup>27,28</sup> and this method was employed here. In the case of the xylyl-based compound, 1,3-di(2-pyridyl)-4,6-dimethylbenzene (dpyxH), the starting haloaromatic is 1,3-dibromo-4,6-dimethylbenzene, which was readily prepared by dibromination of *m*-xylene with bromine in the presence of a catalytic amount of iodine (Scheme 2).<sup>29</sup>

**2.2.  $C\wedge N\wedge O$  Ligands.** The Hantzsch pyridine synthesis or its variants are appropriate for the formation of 6-aryl-2-picolinic acid derivatives. Thus, 4-*p*-tolyl-6-phenylpicolinic acid (tppicH<sub>2</sub>) was prepared by a classical Kröhnke condensation<sup>30</sup> of 2-oxo-4-*p*-tolyl-but-3-enoic acid with 1-(2-oxo-2-phenylethyl)pyridinium iodide and ammonium acetate (Scheme 2).<sup>31</sup>

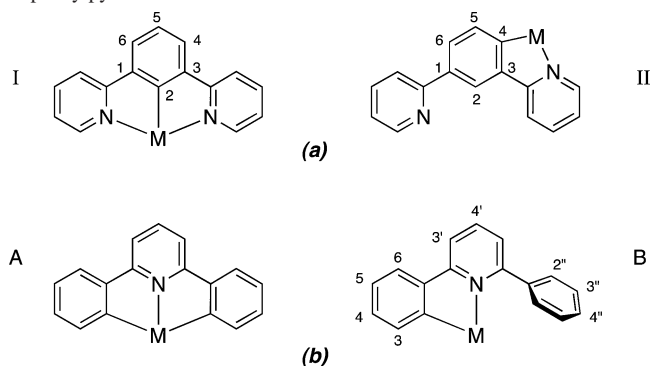
**2.3.  $C\wedge N\wedge C$  Ligands.** Since such ligands also feature a central pyridine ring, a Hantzsch-type synthesis might again be anticipated to be appropriate, as used by Kröhnke in the

- (23) Mamo, A.; Stefio, I.; Parisi, M. F.; Credi, A.; Venturi, M.; Di Pietro, C.; Campagna, S. *Inorg. Chem.* **1997**, *36*, 5947.  
 (24) Slinker, J.; Bernards, D.; Houston, P. L.; Abruña, H. D.; Bernhard, S.; Malliaras, G. G. *Chem. Commun.* **2003**, 2393.  
 (25) Wilkinson, A. J.; Goeta, A. E.; Foster, C. E.; Williams, J. A. G. *Inorg. Chem.* **2004**, *43*, 6513.

- (26) (a) Yutaka, T.; Obara, S.; Ogawa, S.; Nozaki, K.; Ikeda, N.; Ohno, T.; Ishii, Y.; Sakai, K.; Haga, M. *Inorg. Chem.* **2005**, *44*, 4737. (b) Haga, M.; *Oral Communication*, 16<sup>th</sup> International Symposium on the Photochemistry and Photophysics of Coordination Compounds; Asilomar, 2006.  
 (27) Beley, M.; Chodorowski, S.; Collin, J.-P.; Sauvage, J.-P. *Tetrahedron Lett.* **1993**, *34*, 2933.  
 (28) Cárdenas, D. J.; Echavarren, A. M.; Ramirez de Arellano, M. C. *Organometallics* **1999**, *18*, 3337.  
 (29) The method used was a modification of that described in Allinson, G.; Bushby, R. J.; Jesudason, M. V.; Paillaud, J. L.; Taylor, N. J. *Chem. Soc., Perkin Trans. 2* **1997**, 147.  
 (30) Kröhnke, F. *Synthesis* **1976**, 1.  
 (31) Baba, A.; Wang, W.; Yong, K. W.; Strong, L.; Schmehl, R. H. *Synth. Comm.* **1994**, *24*, 1029. Kipp, R. A.; Li, Y.; Simon, J. A.; Schmehl, R. H. *J. Photochem. Photobiol. A* **1999**, *121*, 27.



**Scheme 3.** (a) N $\wedge$ C $\wedge$ N and N $\wedge$ C Binding Modes of 2,6-Dipyridylbenzene. (b) C $\wedge$ N $\wedge$ C and C $\wedge$ N Binding Modes of 2,6-Diphenylpyridine



formation of 2,6-diphenylpyridine.<sup>30</sup> However, this method proved to be unsuitable for the formation of the fluorinated derivative F<sub>4</sub>dppyH<sub>2</sub>. Competitive nucleophilic aromatic substitution was observed during the formation of the requisite enamionone—the reaction of dimethylamine and formaldehyde with 2,4-difluoroacetophenone—with dimethylamine replacing one or more fluorine atoms. Instead, this ligand was prepared by Suzuki cross-coupling of 2,4-difluorophenylboronic acid with 2,6-dibromopyridine (Scheme 2).

**3. Synthesis of the Iridium Complexes. 3.1. Chloro-Bridged Iridium Dimers and [Ir(N $\wedge$ C $\wedge$ N)(N $\wedge$ N $\wedge$ N)]<sup>2+</sup> Complexes. 3.1.1. N $\wedge$ C $\wedge$ N = 1,3-Di(2-pyridyl)benzene (dpyb) and Its Associated Problems.** Our initial investigations centered on the attempted complexation of 1,3-di(2-pyridyl)benzene (dpybH) to iridium(III) as a terdentate, N $\wedge$ C $\wedge$ N-coordinating ligand (Scheme 3a, binding mode I). Binding of dpyb in such a manner has previously been observed for the neighboring transition metals Ru(II),<sup>32</sup> Os(II),<sup>32a,b</sup> and Pt(II).<sup>28,33</sup> Cyclometalation of iridium(III) is commonly performed in a mixture of 2-ethoxyethanol and water, for example, in the preparation of chloro-bridged dinuclear iridium complexes such as [Ir(ppy)<sub>2</sub>( $\mu$ -Cl)]<sub>2</sub>.<sup>6</sup> Reaction of dpybH with IrCl<sub>3</sub>·3H<sub>2</sub>O at 130 °C in this solvent system (3:1 by volume) resulted in an orange precipitate, but <sup>1</sup>H NMR spectroscopy in *d*<sub>6</sub>-DMSO revealed a complex mixture of cyclometalated products, purification of which was hindered by the low solubility in all common solvents. The product mixture was therefore reacted directly with 4'-(*p*-tolyl)-2,2':6',2''-terpyridine (ttpy) in ethylene glycol at reflux<sup>34</sup> on the grounds that the resulting products could shed light on its composition. A very small amount of the anticipated product [Ir(dpyb)(ttpy)]<sup>2+</sup> (Scheme 4) was ob-

tained following chromatographic separation (1% yield), containing dpyb bound in the desired N $\wedge$ C $\wedge$ N-coordinating manner. Other products isolated and identified by electrospray mass spectrometry and <sup>1</sup>H NMR spectroscopy were [Ir(dpyb-*N,C*<sup>4</sup>)(ttpy-*N,N,N*)Cl]<sup>+</sup> and [Ir(dpyb-*N,C*<sup>4</sup>)<sub>2</sub>(ttpy-*N,N,N*)]<sup>+</sup> (Scheme 4), where cyclometalation had occurred through the C<sup>4</sup> position of the phenylene ring (Scheme 3a, binding mode II). Thus, we may postulate that the orange solid from the initial reaction of dpybH with IrCl<sub>3</sub>·3H<sub>2</sub>O contains at least the three species shown bracketed in the center of Scheme 4. The predominance of the bidentate N,C<sup>4</sup> coordination over N,C<sup>2</sup>,N may be related to the fact that the C<sup>2</sup> position is more sterically hindered by the pyridyl rings, with metalation of the substitutionally inert iridium(III) ion likely to be kinetically favored at the C<sup>4</sup> position. A similar coordination mode has been observed upon direct reaction of dpybH with palladium acetate, leading to a dimeric species dipalladated at C<sup>4</sup> and C<sup>6</sup>.<sup>28</sup>

**3.1.2. N $\wedge$ C $\wedge$ N = 1,3-di(2-pyridyl)-4,6-dimethylbenzene (dpyx) and Its Major Advantages.** To favor the desired terdentate coordination mode, this competitive cyclometalation at the C<sup>4</sup> and C<sup>6</sup> positions was blocked by the introduction of methyl substituents into the ligand to give dpyxH (Scheme 2). Reaction of dpyxH with IrCl<sub>3</sub>·3H<sub>2</sub>O in ethoxyethanol/water (3:1) at 80 °C again led to a yellow-orange solid. Although the solid is insoluble in most common solvents, a <sup>1</sup>H NMR spectrum could be obtained in *d*<sub>6</sub>-DMSO following heating and exhibited the same C<sub>2</sub> symmetry as the free ligand, but with the loss of the phenylene proton signal between the two pyridyl rings (H<sup>2</sup> in ligand,  $\delta$  = 7.43 ppm). As expected for cyclometalation at this carbon, a significant upfield shift of the resonance of the proton para to this position is also observed (from 7.26 to 6.98 ppm). An X-ray diffraction study of a single crystal obtained from DMSO solution revealed the structure to be [Ir(dpyx)(DMSO)Cl<sub>2</sub>] (Figure 1). The desired N $\wedge$ C $\wedge$ N coordination is evident, with a sulfur-bound DMSO molecule trans to the metalated carbon. The unambiguous identification of the initially formed solid is apparently thus not possible by crystallography or <sup>1</sup>H NMR spectroscopy, but MALDI mass spectrometry suggests that it is the chloride-bridged dimer [Ir(dpyx)Cl( $\mu$ -Cl)]<sub>2</sub> (*m/z* = 1044) (structure 1 in Scheme 5), which then undergoes cleavage of the bridging chlorides upon solvation in DMSO. Such chloride bridge cleavage is well-established for dinuclear cyclometalated complexes of the type [Ir(ppy)<sub>2</sub>( $\mu$ -Cl)]<sub>2</sub> and [Pt(ppy)( $\mu$ -Cl)]<sub>2</sub>.<sup>6,35,36</sup>

In the structure of [Ir(dpyx)(DMSO)Cl<sub>2</sub>] (Figure 1; henceforth denoted **1-DMSO**), the iridium(III) center exhibits a distorted octahedral geometry due to the geometric constraints of the terdentate binding of dpyx. The two Ir–Cl bonds are approximately perpendicular to the plane of the dpyx ligand, with the sulfur-bound DMSO molecule occupying the remaining coordination site of the iridium(III)

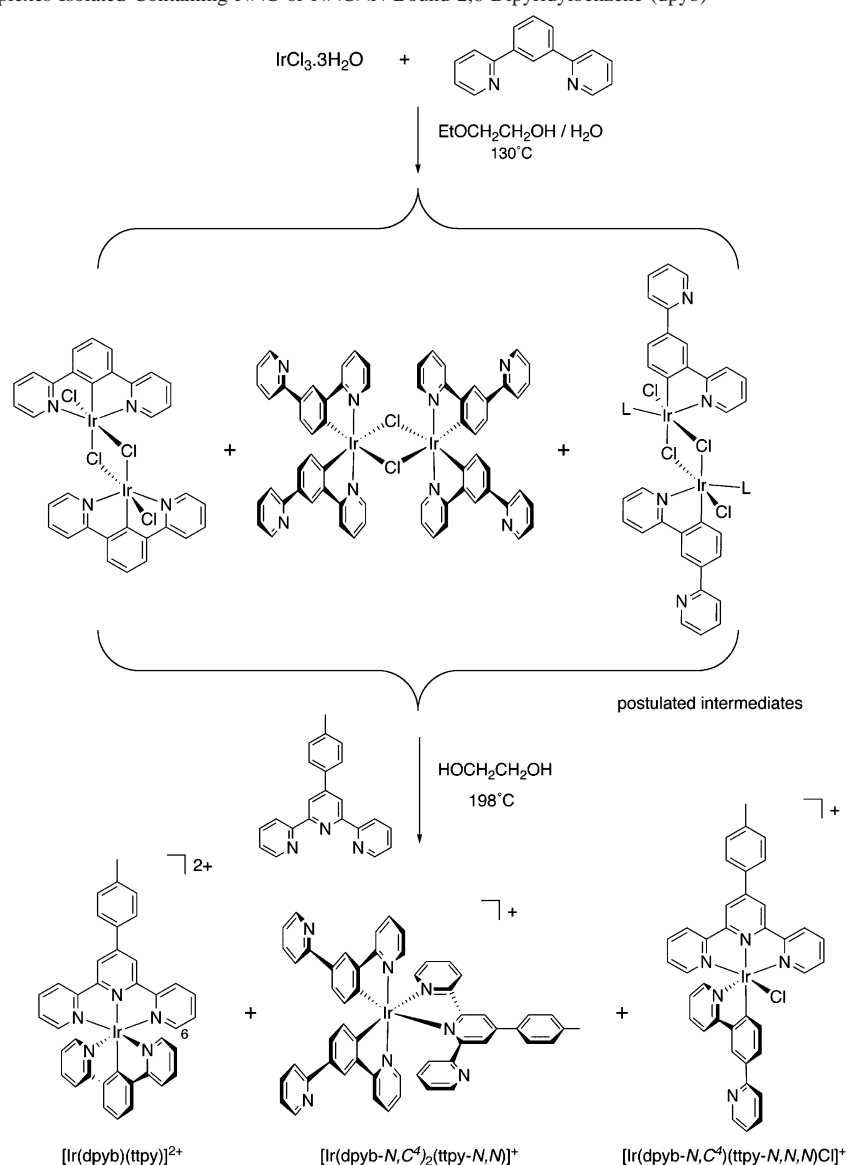
(32) (a) Barigelletti, F.; Flamigni, L.; Guardigli, M.; Juris, A.; Beley, M.; Chodorowski-Kimmes, S.; Collin, J.-P.; Sauvage, J.-P. *Inorg. Chem.* **1996**, *35*, 136. (b) Barigelletti, F.; Flamigni, L.; Collin, J.-P.; Sauvage, J.-P. *Chem. Commun.* **1997**, 333. (c) Patoux, C.; Launay, J.-P.; Beley, M.; Chodorowski-Kimmes, S.; Collin, J.-P.; James, S.; Sauvage, J.-P. *J. Am. Chem. Soc.* **1998**, *120*, 3717.

(33) (a) Williams, J. A. G.; Beeby, A.; Davies, E. S.; Weinstein, J. A.; Wilson, C. *Inorg. Chem.* **2003**, *42*, 8609. (b) Farley, S. J.; Rochester, D. L.; Thompson, A. L.; Howard, J. A. K.; Williams, J. A. G. *Inorg. Chem.* **2005**, *44*, 9690.

(34) Such forcing conditions (ethylene glycol at 196 °C) have previously been found necessary for the introduction of terpyridines into the coordination sphere of iridium: see refs 8 and 9.

(35) Neve, F.; Crispini, A.; Campagna, S.; Serroni, S. *Inorg. Chem.* **1999**, *38*, 2250.

(36) For example: (a) Kvam, P.-I.; Songstad, J. *Acta Chem. Scand.* **1995**, *49*, 313. (b) Balashev, K. P.; Puzyk, M. V.; Kotlyar, V. S.; Kulikova, M. V. *Coord. Chem. Rev.* **1997**, *159*, 109.

**Scheme 4.** Iridium Complexes Isolated Containing N $\wedge$ C or N $\wedge$ C $\wedge$ N-Bound 2,6-Dipyridylbenzene (dpyb)<sup>a</sup>

<sup>a</sup> In the third of the postulated intermediates, L is likely to be a monodentate neutral ligand, for example, monodentate N-bound dpybH.

center. Selected bond lengths and angles are listed in Table 1. The Ir–C bond {1.976(4) Å} is shortened with respect to the analogous bonds in *fac*-[Ir(mppy)<sub>3</sub>] {2.024(6) Å; mppy = 2-(4'-methylphenyl)pyridine},<sup>37</sup> a result of the constraints imposed by binding of two flanking pyridine rings. The Ir–N distances of [Ir(dpyx)(DMSO)Cl<sub>2</sub>] {2.067(3) and 2.087(3) Å} are also shortened with respect to those in *fac*-[Ir(mppy)<sub>3</sub>] {2.132(5) Å}, attributable to the strong trans influence of the cyclometalated carbons opposite the nitrogen atoms in the latter.

Reaction of [Ir(dpyx)Cl(μ-Cl)]<sub>2</sub> (**1**) with 4'-tolyl-terpyridine (ttpy) in ethylene glycol at 196°C for 45 min gave [Ir(dpyx)(ttpy)]<sup>2+</sup> cleanly in 87% yield (Scheme 5, compound **2b**), a huge improvement over that achieved for [Ir(dpyb)(ttpy)]<sup>2+</sup>. Similarly, reaction with unsubstituted terpyridine (tpy) readily gave [Ir(dpyx)(tpy)]<sup>2+</sup> (**2a**), confirming the generality of this new class of complex.<sup>38</sup>

**3.2. [Ir(N $\wedge$ C $\wedge$ N)(C $\wedge$ N $\wedge$ C)] Complexes: [Ir(dpyx)-(dppy)] (**3**) and [Ir(dpyx)(F<sub>4</sub>dppy)] (**4**).** The application of the N $\wedge$ C $\wedge$ N-bound iridium(III) precursor compound, **1**, to the synthesis of the charge-neutral complex [Ir(dpyx)(dppy)] (**3**) was investigated. Reaction with 2,6-diphenylpyridine (dppyH<sub>2</sub>) in refluxing ethylene glycol for up to 1 h—conditions which led to the efficient formation of the [Ir(dpyx)(N $\wedge$ N $\wedge$ N)]<sup>2+</sup> complexes—gave none of the desired product. Although <sup>1</sup>H NMR spectroscopy of the fractions containing the dpyx ligand isolated from chromatography showed that it was still bound in an N $\wedge$ C $\wedge$ N manner, no other aromatic proton resonances could be observed, and electrospray ionization mass spectrometry suggested that the remaining three coordination sites were occupied by weakly bound solvent molecules. In contrast, reaction for 24 h under the same conditions did allow the chromatographic isolation

(38) The X-ray crystal structure of a representative member, [Ir(dpyx)(ttpy)](PF<sub>6</sub>)<sub>2</sub>, was described in our preliminary communication (ref 25) and showed the anticipated pseudo-octahedral geometry at the metal, with the two ligands occupying mutually orthogonal planes.

(37) Garces, F. O.; Dedeian, K.; Keder, N. L.; Watts, R. J. *Acta Crystallogr., Sect. C: Cryst. Struct. Commun.* **1993**, *49*, 1117.

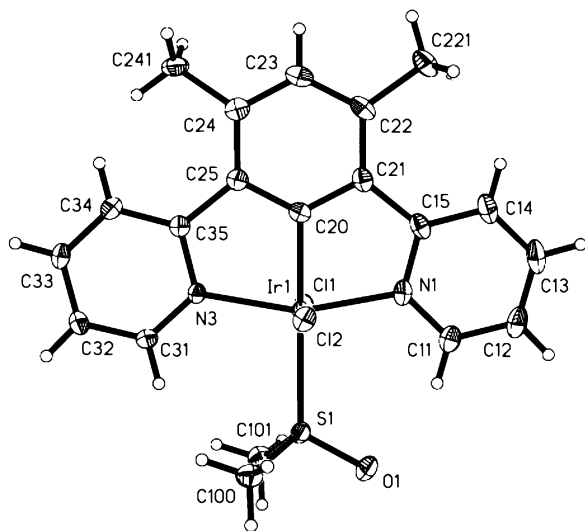


**Figure 1.** Structure of  $[\text{Ir}(\text{dpyx})(\text{DMSO})\text{Cl}_2]$  (**1-DMSO**) crystallized from DMSO;  $T = 120$  K; thermal ellipsoids shown at the 30% probability level.

of a dppyH-containing iridium(III) complex. However,  $^1\text{H}$  NMR spectroscopy showed clearly that this ligand was only bidentately bound ( $\text{C}\wedge\text{N}$  coordination), with the remaining phenyl group unbound (mode B in Scheme 3b). The same product could also be obtained at lower temperatures if the reaction was carried out in the presence of  $\text{Ag}^+$  salts to promote dechlorination, e.g., in ethanol at reflux for 6 days.

The identity of the ligand L in the sixth coordination site, if there is one, remains ambiguous, but is most likely a weakly bound solvent molecule. Thus, electrospray mass spectrometry reveals only the mass of the species  $[\text{Ir}(\text{dpyx})(\text{dppyH})]^+$ , even at the lowest ionization cone voltages.  $\text{C}_2$  symmetry is observed in the resonances of the unbound phenyl ring in the  $^1\text{H}$  NMR spectrum, while the  $^1\text{H}-^1\text{H}$  NOESY reveals a through-space interaction between the *o*-phenyl protons ( $\text{H}''$ , see Scheme 3b) and those adjacent to the nitrogen of the pyridyl rings of dpyx ( $\text{H}^6$ ). These observations indicate that the unbound phenyl is free to rotate and to occupy a plane orthogonal to the rest of the dppyH ligand. This contrasts with the work of Crabtree et al. on cyclometalation of iridium phosphine species, where 2,6-diphenylpyridine gave a mono-cyclometalated species  $[\text{Ir}(\text{dppyH}-N, \text{C}^2)(\text{PPh}_3)_2\text{H}]^+$ , in which the sixth site of the metal was stabilized by an agostic bond to the noncyclometalated phenyl ring.<sup>39</sup> In a related system containing cyclometalated 2-isopropylbenzoquinolines, such an agostic interaction was sterically disfavored, and the site opposite to metalation remained empty.<sup>40</sup> Such a possibility cannot be ruled out in the present instance.

The desired complex **3**, containing the bis-cyclometalated dppy ligand, was eventually obtained by using molten dppyH<sub>2</sub> itself as the reaction solvent (mp = 74–76 °C).<sup>41</sup> Thus, heating **1** with silver trifluoromethanesulfonate in molten dppyH<sub>2</sub> at 110 °C in the absence of any other solvent, followed by chromatographic purification, led to the desired

complex as an orange solid in 37% yield. Similarly, reaction with  $\text{F}_4\text{dppyH}_2$  (mp = 83–84 °C) under similar conditions led to the fluorinated complex **4**, a yellow solid, in 21% yield. Unfortunately, neither complex is amenable to scale-up; in the first case, because of the inherent instability of the product in solution (see below), and in the second, because of the need for large excess quantities of the  $\text{F}_4\text{dppyH}_2$  ligand (if the ratio of ligand to intermediate is reduced, the mixture no longer melts below 110 °C and yields are greatly decreased, while the use of higher temperatures leads to decomposition). Preparation of the dithienyl analogue  $[\text{Ir}(\text{dpyx})(\text{dthpy})]$  was attempted in a similar manner, but no evidence of complexation was observed in this case, nor when the reaction was carried out in refluxing ethylene glycol. The use of acetic acid as the solvent led to isolation of  $[\text{Ir}(\text{dpyx})(\text{dthpyH})]^+$  (**6**), which contains the bidentate  $\text{C}\wedge\text{N}$ -coordinated dthpyH ligand (Scheme 5). Again, the identity of the ligand in the sixth site remains ambiguous.

**3.3.  $[\text{Ir}(\text{N}\wedge\text{C}\wedge\text{N})(\text{C}\wedge\text{N})\text{Cl}]$  Complex:  $[\text{Ir}(\text{dpyx})(\text{ppy})\text{Cl}]$  (**5**).** Heating **1** in 2-phenylpyridine (ppyH) in the presence of  $\text{AgOTf}$  gave the complex  $[\text{Ir}(\text{dpyx})(\text{ppy})\text{Cl}]$  (**5**) in good yield. There are two possible isomers of this complex, with either a meridional or facial arrangement of the nitrogen atoms. The  $^1\text{H}-^1\text{H}$  NOESY spectrum shows a cross-peak between  $\text{H}^6$  of dpyx and  $\text{H}^6$  of ppy, indicative of the *mer* complex. This is expected to be the thermodynamically favored product, because the high trans influence of the cyclometalated carbons will disfavor the alternative in which the carbon atoms would be disposed trans to one another.

**3.4.  $[\text{Ir}(\text{N}\wedge\text{C}\wedge\text{N})(\text{C}\wedge\text{N}\wedge\text{O})]$  Complexes:  $[\text{Ir}(\text{dpyx})(\text{tppic})]$  (**7**) and  $[\text{Ir}(\text{dpyx})(\text{hbqc})]$  (**8**).** The picolinic acid derivatives tppicH<sub>2</sub> and hbqcH<sub>2</sub> have high melting points, rendering a solvent-free approach to complexation unsuitable. Molten benzoic acid was selected as the reaction medium, owing to its appropriate melting point (122–123 °C) and potential for solubilizing pyridine-carboxylic acid functionalized ligands. Thus, reaction of **1** with the respective ligand in the presence of  $\text{AgOTf}$  in benzoic acid led to the complexes  $[\text{Ir}(\text{dpyx})(\text{tppic})]$  (**7**) and  $[\text{Ir}(\text{dpyx})(\text{hbqc})]$  (**8**) in good yield. Interestingly, all attempts to prepare a related charge-neutral complex containing the  $\text{O}\wedge\text{N}\wedge\text{O}$ -coordinating ligand, 2,6-dipyridinecarboxylate, in place of the  $\text{C}\wedge\text{N}\wedge\text{O}$  ligand, were unsuccessful, leading to a complex mixture of inseparable products.

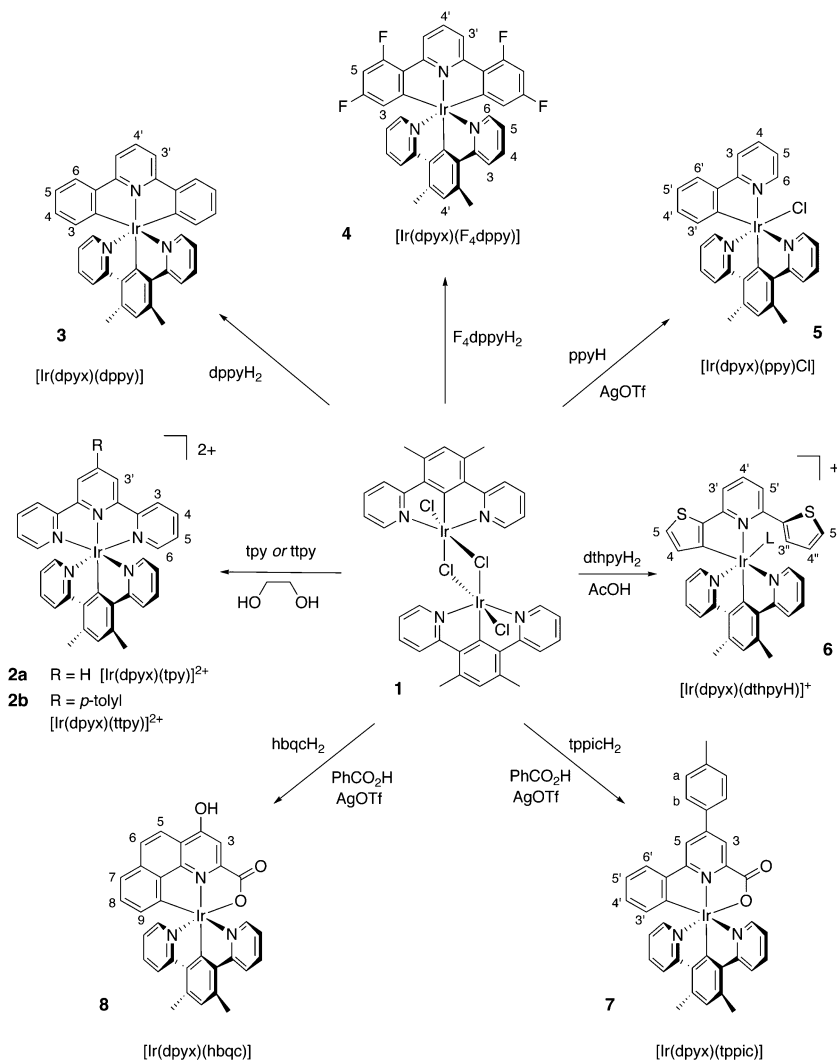
**4. Photophysical Properties. 4.1.  $[\text{Ir}(\text{N}\wedge\text{C}\wedge\text{N})(\text{C}\wedge\text{N}\wedge\text{C})]$  Complexes:  $[\text{Ir}(\text{dpyx})(\text{dppy})]$  (**3**) and  $[\text{Ir}(\text{dpyx})(\text{F}_4\text{dppy})]$  (**4**).**  
**4.1.1. Ground-State Absorption.** The absorption spectra of **3** and **4** in acetonitrile solution at room temperature show very intense bands in the near-UV region between 240 and 300 nm (Figure 2, Table 2). By comparison with the well-established literature data for *fac*- $[\text{Ir}(\text{ppy})_3]$ , these are assigned to spin-allowed  $^1\pi-\pi^*$  transitions of the ligands.<sup>6,16</sup> A series of weaker, lower-energy features extending well

(39) Albéniz, A. C.; Schulte, G.; Crabtree, R. H. *Organometallics* **1992**, *11*, 242.

(40) Clot, E.; Eisenstein, O.; Dubé, T.; Faller, J. W.; Crabtree, R. H. *Organometallics* **2002**, *21*, 575.

(41) Several other solution-based syntheses were also attempted using a variety of solvents: ethoxyethanol/water, acetic acid, toluene, and glycerol, in each case, both in the presence and absence of silver ions. These reactions led either to intractable mixtures or, at best, to evidence of products containing  $\text{N}\wedge\text{C}$ -bound diphenylpyridine, after chromatographic purification.

**Scheme 5.** Structures of the Iridium Complexes Isolated, Containing the N $\wedge$ C $\wedge$ N-Bound Ligand dpyx, Obtained through the Intermediacy of [Ir(dpyx)Cl( $\mu$ -Cl)]<sub>2</sub> (**1**)<sup>a</sup>



<sup>a</sup> The numbering system used in the <sup>1</sup>H NMR assignments of the complexes is included; the numbering of the dpyx ligand in [Ir(dpyx)(F<sub>4</sub>dppy)] is representative of all the complexes.

**Table 1.** Selected Bond Lengths (Å) and Angles (deg) for [Ir(dpyx)(DMSO)Cl<sub>2</sub>] (**1**-DMSO)

Ir–N(1)	2.067(3)	C(20)–Ir–S(1)	178.66(10)
Ir–N(3)	2.087(3)	C(20)–Ir–N(1)	80.00(13)
Ir–C(20)	1.976(4)	N(1)–Ir–N(3)	159.89(12)
Ir–Cl(1)	2.352(2)	C(20)–Ir–Cl(1)	90.94(11)
Ir–Cl(2)	2.374(2)	N(1)–Ir–Cl(2)	89.29(9)
Ir–S(1)	2.438(2)	Cl(1)–Ir–Cl(2)	176.20(3)

into the visible region are attributable to both allowed and spin-forbidden metal-to-ligand charge transfer (<sup>1,3</sup>MLCT) bands. It is clear that the bis-terdentate complexes show significantly lower energy MLCT bands than *fac*- and *mer*-[Ir(ppy)<sub>3</sub>] (which exhibit similar absorbance spectra to one another), an effect which may be attributed to a lowering in energy of the acceptor ligand π\* orbitals (LUMO) upon increased delocalization across the three aromatic rings of the N $\wedge$ C $\wedge$ N ligand. The MLCT transitions of the fluorinated complex **4** are blue-shifted with respect to **3**, which may be readily rationalized in terms of the stabilization of the HOMO as a result of the electron-withdrawing nature of the fluorine substituents (*vide infra*).

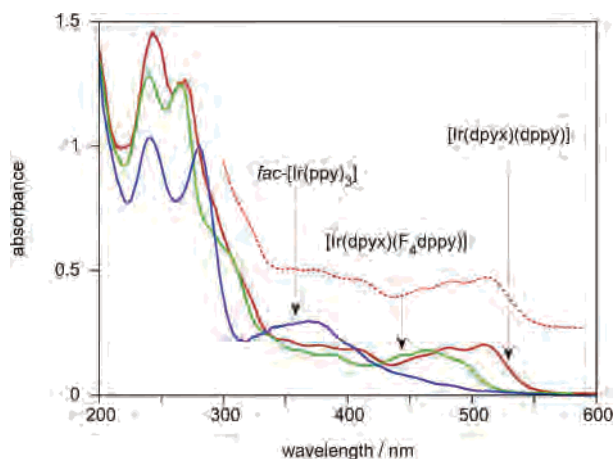


**Figure 2.** Absorption spectra of [Ir(dpyx)(dppy)] (**3**) (red) and [Ir(dpyx)(F<sub>4</sub>dppy)] (**4**) (green) in CH<sub>3</sub>CN at 295K, together with the spectrum of *fac*-[Ir(ppy)<sub>3</sub>] (blue) for comparison. The low-energy portion of the excitation spectrum of [Ir(dpyx)(dppy)], registered at 600 nm under the same conditions, is also shown (red dotted line).

**4.1.2. Emission.** Both of the new complexes are strongly luminescent in degassed solution, displaying a single, broad,

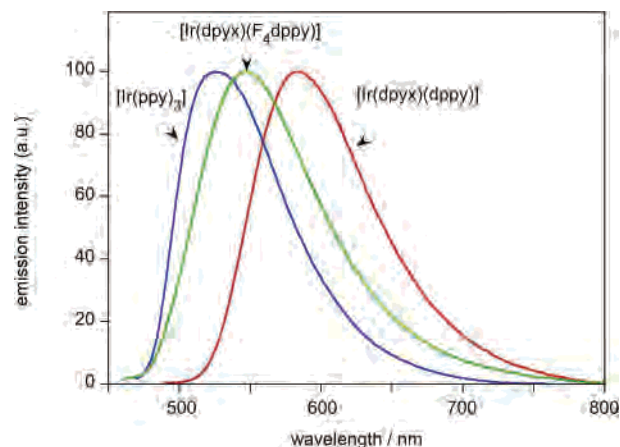


**Table 2.** Absorption Data for the Iridium Complexes in Acetonitrile Solution at 295 K

complex	absorption $\lambda_{\max}/\text{nm}$ ( $\epsilon/\text{mol}^{-1} \text{ dm}^3 \text{ cm}^{-1}$ )
[Ir(dpyx)(DMSO)Cl <sub>2</sub> ] <b>1-DMSO</b>	286 (20 500), 388 (6100), 426sh (2020), 494 (455)
[Ir(dpyx)(tpy)] <sup>2+</sup> <b>2a</b>	261 (38 500), 270 (35 300), 298br (26 000), 335sh (13 100), 377 (10 100), 435 (700), 465 (500)
[Ir(dpyx)(tppy)] <sup>2+</sup> <b>2b</b>	264 (52 900), 283 (45 100), 301 (39 900), 361 (20 300), 377 (21 600), 435 (1500), 463 (1000)
[Ir(dpyx)(dppy)] <b>3</b>	244 (53 900), 269 (46 900), 349 (7700), 378 (6900), 406 (6500), 458 (5500), 481 (6800), 510 (7300)
[Ir(dpyx)(F <sub>4</sub> dppy)] <b>4</b>	240 (49 200), 265 (48 000), 290sh (24 800), 304sh (21 200), 334 (8400), 360 (6000), 385 (5600), 447 (5600), 464 (6400), 487 (5200)
[Ir(dpyx)(ppy)Cl] <b>5</b>	239 (44 700), 258 (39 700), 285 (37 000), 353 (6200), 369 (7800), 399 (10 000), 417 (11 300), 455 (3600), 492 (1300)
[Ir(dpyx)(tppic)] <b>7</b>	242 (32 800), 273 (35 700), 337 (13 500), 393 (6900), 429 (6700), 459 (4300), 489 (1700)
[Ir(dpyx)(hbqc)] <b>8</b>	245 (34 500), 290 (16 600), 315sh (10 400), 341 (6500), 363 (5900), 393 (4900), 428 (4600), 459 (2800), 492 (1100)

structureless emission band, typical of phosphorescence from a <sup>3</sup>MLCT state (Figure 3, Table 3). This assignment is broadly supported by DFT calculations, which confirm that the LUMO is localized almost exclusively on the N $\wedge$ C $\wedge$ N-coordinating ligand, while the HOMO comprises a significant contribution from the metal: contour plots of the frontier orbitals are shown in Figure 4, and further details are provided in the Supporting Information. The two ligands are seen to make a significant contribution to the HOMO, as well as the metal, and so the excited state is perhaps best regarded as having mixed d(Ir)/ $\pi$ (dpyx)/ $\pi$ (dppy)  $\rightarrow$   $\pi^*$ (dpyx) character. Similar conclusions regarding the contribution of ligand-centered (LC) and, for heteroleptic complexes, ligand-to-ligand charge transfer (LLCT) character to the emissive excited state have been reached in DFT studies of related iridium complexes.<sup>22,42</sup>

The luminescence of **3** ( $\lambda_{\max} = 585 \text{ nm}$ ) is substantially red-shifted with respect to that of *fac*-[Ir(ppy)<sub>3</sub>] ( $\lambda_{\max} = 528 \text{ nm}$ ). As in absorption, this is attributed to a lowering of the N $\wedge$ C $\wedge$ N ligand  $\pi^*$  orbital energy upon the increased conjugation which accompanies the introduction of an additional pyridyl ring compared to ppy. The blue-shift of the emission band upon 4,6-difluorination (**4**,  $\lambda_{\max} = 547 \text{ nm}$ ), which mirrors the effect in absorption, may be attributed to a greater stabilization of the HOMO compared to the LUMO upon introduction of the inductively electron-withdrawing fluorine atoms. The molecular orbital plots from the DFT calculations substantiate this interpretation since the LUMO is seen to be almost entirely localized on the unsubstituted dpyx ligand—and hence should not be significantly affected by substituents in the dppy ligand—while the HOMO has a significant contribution from the dppy moiety. Hypsochromic shifts have also been reported for *fac*-[Ir(4,6-dfppy)<sub>3</sub>] compared to *fac*-[Ir(ppy)<sub>3</sub>],<sup>43</sup> [Ir(4,6-dfppy)<sub>2</sub>(N $\wedge$ N)]<sup>n+</sup>

(42) Hay, P. J. *J. Phys. Chem. A* **2002**, *106*, 1634.(43) Tamayo, A. B.; Alleyne, B. D.; Djurovich, P. I.; Lamansky, S.; Tsyba, I.; Ho, N. N.; Bau, R.; Thompson, M. E. *J. Am. Chem. Soc.* **2003**, *125*, 7377.**Figure 3.** Emission spectra of [Ir(dpyx)(dppy)] (**3**) (red) and [Ir(dpyx)(F<sub>4</sub>dppy)] (**4**) (green) in CH<sub>3</sub>CN at 295 K, following excitation into the lowest energy absorption band, together with the spectrum of *fac*-[Ir(ppy)<sub>3</sub>] (blue) for comparison.

compared to [Ir(ppy)<sub>2</sub>(N $\wedge$ N)]<sup>n+</sup>,<sup>18e19d,44</sup> and [Pt(4,6-dfppy)-(acac)] compared to [Pt(ppy)(acac)],<sup>45</sup> traced back in each case to the influence of the fluorine atoms on the HOMO {4,6-dfppy = 2-(4,6-difluorophenyl)pyridine; N $\wedge$ N = a 2,2'-bipyridine ligand ( $n = 1$ ) or 2-triazolylpyridine ( $n = 0$ )}.

The relatively long luminescence lifetimes,  $\tau$ , of the complexes, 3.7–3.8  $\mu\text{s}$  in degassed solution at ambient temperature (Table 3), are also suggestive of significant ligand-centered character in the excited state, as opposed to the rather shorter lifetimes typical of more purely MLCT states.<sup>7,43,45</sup> The emission is quenched strongly by dissolved molecular oxygen, with bimolecular rate constants of quenching  $k_Q$  of the order of  $6 \times 10^9 \text{ M}^{-1} \text{ s}^{-1}$  (Table 3).

The luminescence quantum yields ( $\phi$ ) of **3** and **4** in degassed acetonitrile solution are 0.21 and 0.41, respectively. Assuming that formation of the emissive state occurs with unity efficiency, one may calculate an estimate of the unimolecular radiative ( $k_r$ ) and nonradiative ( $\sum k_{nr}$ ) decay rate constants by application of eqs 1 and 2:

$$\tau = 1/(k_r + \sum k_{nr}) \quad (1)$$

$$\phi = k_r/(k_r + \sum k_{nr}) = k_r \cdot \tau \quad (2)$$

Inspection of the parameters so obtained (Table 3) confirms that the higher emission quantum yield of the fluorinated complex compared to the parent is due both to a higher radiative rate constant and to reduced nonradiative decay, consistent with the predictions of the energy gap law: for a homologous series of complexes, a decrease in the emissive excited state energy is typically accompanied by a decrease in  $\phi$ .<sup>46</sup>

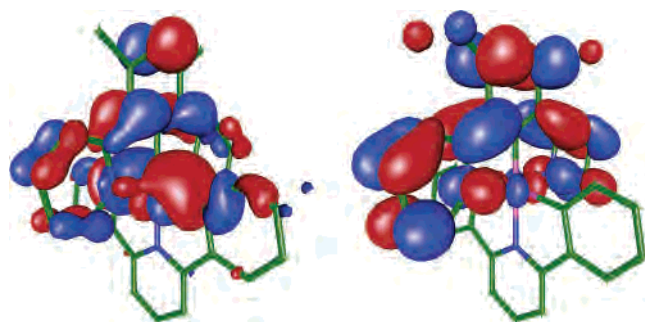
(44) Welter, S.; Lafolet, F.; Cecchetto, E.; Vergeer, F.; De Cola, L. *ChemPhysChem* **2005**, *6*, 2417.(45) Brooks, J.; Babayan, Y.; Lamansky, S.; Djurovich, P. I.; Tsyba, I.; Bau, R.; Thompson, M. *Inorg. Chem.* **2002**, *41*, 3055.(46) Englman, R.; Jortner, J. *Mol. Phys.* **1970**, *18*, 145. For an example of the application of the law to metal-complex-doped light-emitting polymers, see: Wilson, J. S.; Chawdhury, N.; Al-Mandhary, M. R. A.; Younus, M.; Khan, M. S.; Raithby, P. R.; Köhler, A.; Friend, R. H. *J. Am. Chem. Soc.* **2001**, *123*, 9412.



**Table 3.** Luminescence Data for the Iridium Complexes in CH<sub>3</sub>CN Solution at 295K, and Corresponding Data for the *fac*- and *mer*-isomers of [Ir(ppy)<sub>3</sub>] and [Ir(4,6-dfppy)<sub>3</sub>] in CH<sub>2</sub>Cl<sub>2</sub>

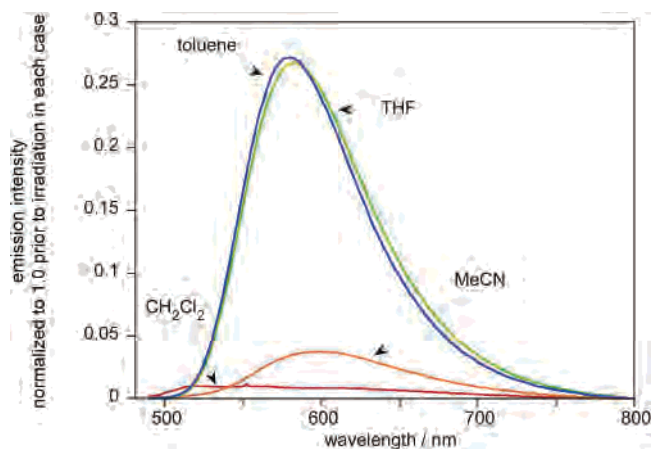
complex	$\lambda_{\text{max}}/\text{nm}$	$\tau$ degassed (aerated)/ns <sup>a</sup>	$\phi$ degassed (aerated) <sup>b</sup>	$k_r/s^{-1}$ <sup>c</sup>	$\Sigma k_{nr}/s^{-1}$ <sup>c</sup>	$k_Q/M^{-1} s^{-1}$ <sup>d</sup>
[Ir(dpyx)(dppy)] <b>3</b>	585	3800 (77)	0.21 (0.0013)	$5.5 \times 10^4$	$2.1 \times 10^5$	$6.7 \times 10^9$
<i>fac</i> -[Ir(ppy) <sub>3</sub> ] <sup>e,f</sup>	510	1900	0.40	$2.1 \times 10^5$	$3.2 \times 10^5$	—
<i>mer</i> -[Ir(ppy) <sub>3</sub> ] <sup>e</sup>	512	150	0.036	$2.4 \times 10^5$	$6.5 \times 10^6$	—
[Ir(dpyx)(F <sub>4</sub> dppy)] <b>4</b>	547	3700 (<100)	0.41 (0.0036)	$1.1 \times 10^5$	$1.6 \times 10^5$	$>5.1 \times 10^9$
<i>fac</i> -[Ir(4,6-dfppy) <sub>3</sub> ] <sup>e</sup>	450	1600	0.43	$2.7 \times 10^5$	$3.6 \times 10^5$	—
<i>mer</i> -[Ir(4,6-dfppy) <sub>3</sub> ] <sup>e</sup>	460	210	0.053	$2.5 \times 10^5$	$4.5 \times 10^6$	—
[Ir(dpyx)(ppy)Cl] <b>5</b>	508	1600 (<100)	0.76 (0.016)	$4.8 \times 10^5$	$1.5 \times 10^5$	$>4.9 \times 10^9$
[Ir(dpyx)(tppic)] <b>7</b>	603	110 (39)	0.053 (0.0092)	$4.8 \times 10^5$	$8.6 \times 10^6$	$8.7 \times 10^9$
[Ir(dpyx)(hbqc)] <b>8</b>	562	170 (<100)	0.027 (0.0043)	$1.6 \times 10^5$	$5.7 \times 10^6$	$>2.2 \times 10^9$
[Ir(dpyx)(tpy)] <sup>2+</sup> <b>2a</b>	502 <sup>g</sup>	— <sup>h</sup>	<0.001	—	—	—

<sup>a</sup> Lifetime of emission,  $\lambda_{\text{ex}} = 355$  nm. <sup>b</sup> Luminescence quantum yield, measured using [Ru(bpy)<sub>3</sub>]Cl<sub>2(aq)</sub> as the standard ( $\phi = 0.028^{53}$ ). <sup>c</sup> Radiative ( $k_r$ ) and nonradiative ( $\Sigma k_{nr}$ ) rate constants calculated from  $\tau$  and  $\phi$  values; estimated uncertainty  $\pm 20\%$ . <sup>d</sup> Bimolecular rate constant for quenching by O<sub>2</sub>, estimated from  $\tau$  values in degassed and aerated solutions. <sup>e</sup> In CH<sub>2</sub>Cl<sub>2</sub>, from ref 43. <sup>f</sup> The emission wavelength of *fac*-[Ir(ppy)<sub>3</sub>] in CH<sub>3</sub>CN is 528 nm (this work). <sup>g</sup> At 77 K. <sup>h</sup> A reliable lifetime could not be obtained using the available setup, owing to the very low intensity of the emission.

**Figure 4.** Density functional theory (DFT) calculation of the HOMO (left) and LUMO (right) for [Ir(dpyx)(dppy)] (**3**).

A pertinent comparison to make is with the *mer*-[Ir(ppy)<sub>3</sub>] derivatives, which incorporate the same meridional coordination geometry as the new terdentate complexes. The *mer*-ppy complexes display much poorer luminescence efficiencies than their *fac* analogues due to a competing *mer*-to-*fac* photoisomerization process.<sup>43</sup> Thus, while *mer*-[Ir(ppy)<sub>3</sub>] derivatives have similar radiative rate constants to the *fac* isomers, their nonradiative rate constants are more than an order of magnitude greater<sup>43</sup> (Table 3) since the *mer*-to-*fac* photoisomerization offers the excited state an additional nonradiative decay pathway. For **3** and **4**, the nonradiative rate constants are of a comparable magnitude to those for *fac*-[Ir(ppy)<sub>3</sub>] and are not elevated like those of *mer*-[Ir(ppy)<sub>3</sub>], suggesting that photodecomposition processes are not a major pathway of nonradiative decay. Instead, luminescence quantum yields appear to be limited by the rather lower radiative rate constants for these complexes, which are 2–4 times smaller than those of the tris-bidentate systems, possibly associated with the smaller contribution of the metal to the frontier orbitals as discussed above.

**4.1.3. Photodissociation.** Given that the  $\Sigma k_{nr}$  values for the new complexes are not abnormally high (e.g., they are actually smaller than for the photostable *fac*-[Ir(ppy)<sub>3</sub>]), rates of photodecomposition are likely to be low. Nevertheless, a photodissociation process is observed for **3** under UV–vis irradiation. <sup>1</sup>H NMR spectroscopic analysis following irradiation of an acetonitrile solution with a xenon lamp indicated that the major compound formed is [Ir(dpyx)(dppyH)L]<sup>+</sup> (Scheme 3b, dppyH binding mode B), the result of cleavage

**Figure 5.** Emission spectra of [Ir(dpyx)(dppy)] (**3**) in toluene (blue), THF (green), CH<sub>3</sub>CN (orange) and CH<sub>2</sub>Cl<sub>2</sub> (red),  $\lambda_{\text{ex}} = 480$  nm, following intense irradiation for 5 min. All spectra are normalized to a peak intensity of 1.0 prior to irradiation.

of one of the mutually trans Ir–C bonds. Just such a process is likely to be the first step in the photoisomerization of *mer*-Ir(ppy)<sub>3</sub> to the *fac* form. However, the terdentate nature of the ligands in **3** prohibits such an isomerization: a *fac* arrangement is not possible, and the partially dissociated species with bidentately bound dppyH is the result.

The solvent dependence of the rate of photodecomposition was investigated in anhydrous solvents (Figure 5). The observed trend, CH<sub>2</sub>Cl<sub>2</sub> > CH<sub>3</sub>CN > THF  $\approx$  toluene, may be related to the ability of the solvent to solvate the sixth site of the complex or to the acidity of the solvent. Given that a species of the form [Ir(dpyx)(dppyH)]<sup>+</sup> was a persistently troublesome side-product in the preparation of **3**, it is likely that the difficulty in obtaining the latter complex in larger quantities is associated with this instability during purification by column chromatography. On the other hand, in the solid state, the compound is stable indefinitely; the stability when incorporated into an electroluminescent device such as an OLED may, therefore, not necessarily be compromised. Although the fluorinated derivative **4** also photodegrades under prolonged irradiation in solution, the rate is significantly decreased compared to the unsubstituted complex **3**, with a significant proportion of the emission intensity being retained after irradiation for 1 h in acetonitrile solution.

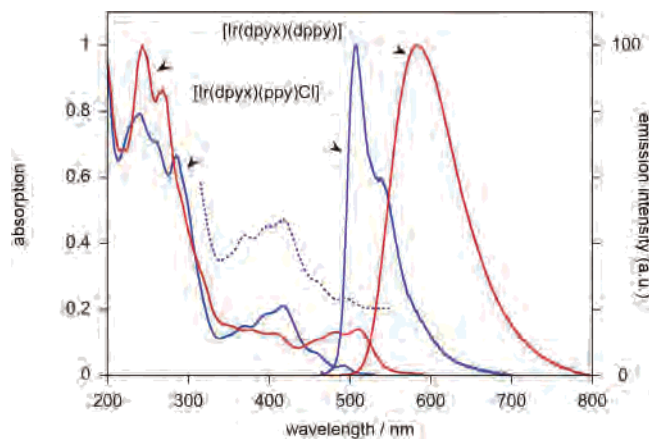


**Figure 6.** Absorption and emission ( $\lambda_{\text{ex}} = 456 \text{ nm}$ ) spectra of  $[\text{Ir}(\text{dpyx})(\text{ppy})\text{Cl}]$  (**5**) in  $\text{CH}_3\text{CN}$  at 295 K (blue solid lines), together with the corresponding spectra of  $[\text{Ir}(\text{dpyx})(\text{dppy})]$  (**3**) for comparison (red lines). The low-energy portion of the excitation spectrum of  $[\text{Ir}(\text{dpyx})(\text{dppy})]$ , registered at 507 nm under the same conditions, is also shown (blue dotted line).

**4.2.  $[\text{Ir}(\text{N}\wedge\text{C}\wedge\text{N})(\text{C}\wedge\text{N})\text{Cl}]$  Complex:  $[\text{Ir}(\text{dpyx})(\text{ppy})\text{Cl}]$  (**5**).** The ground-state absorption spectrum of **5** is shown in Figure 6. As for  $[\text{Ir}(\text{dpyx})(\text{dppy})]$  (also shown in Figure 6 for comparison), the series of bands that extend into the visible region may be assigned to charge-transfer transitions, including the anticipated MLCT bands. They are significantly blue-shifted compared to **3**, which may be rationalized in terms of a lowering of the HOMO energy upon substitution of the second cyclometalating carbon atom of dppy by the much weaker ligand-field chloride ligand. The LUMO is again expected to be localized primarily on the dpyx ligand, such that the introduction of the chloride would be expected to have little effect on the LUMO energy.

**5** is very strongly emissive in solution, exhibiting a significantly blue-shifted spectrum compared to that of  $[\text{Ir}(\text{dpyx})(\text{dppy})]$  (Figure 6). A blue-shift in emission is again consistent with a lowering of the HOMO energy upon substitution of the strong-field cyclometalating carbon by a chloride ligand, without significantly affecting the dpyx-based LUMO. The observation of a more structured emission profile, with a much smaller Stokes' shift ( $600 \text{ cm}^{-1}$  compared to  $2400 \text{ cm}^{-1}$  for  $[\text{Ir}(\text{dpyx})(\text{dppy})]$  in  $\text{CH}_3\text{CN}$  at 295 K) is suggestive of an increase in LC character. Therefore, the emission is assigned to a heavily mixed  $\pi$ -(dpyx)/d(Ir)  $\rightarrow \pi^*(\text{dpyx})$  (LC/MLCT) excited state, reflecting the lowering of the predominantly metal-based HOMO in  $[\text{Ir}(\text{dpyx})(\text{dppy})]$  to an energy similar to that of the dpyx ligand  $\pi$  orbital.

The luminescence quantum yield in degassed acetonitrile solution is outstandingly high,  $\phi = 0.76$ , and among the highest hitherto reported for tris-cyclometalated iridium complexes. The value is significantly higher not only than that of  $[\text{Ir}(\text{dpyx})(\text{dppy})]$  ( $\phi = 0.21$ ), which could be partly expected on the basis of the energy gap law given the difference in  $\lambda_{\text{max}}$ , but also than that of *fac*- $[\text{Ir}(\text{ppy})_3]$  ( $\Phi_{\text{PL}} = 0.40$  in toluene), which has a very similar emission energy. Application of eqs 1 and 2 establishes that this improvement is due to a combination of an increased radiative rate constant ( $k_{\text{r}} = 4.8 \times 10^5 \text{ s}^{-1}$ ) and a decreased nonradiative contribu-

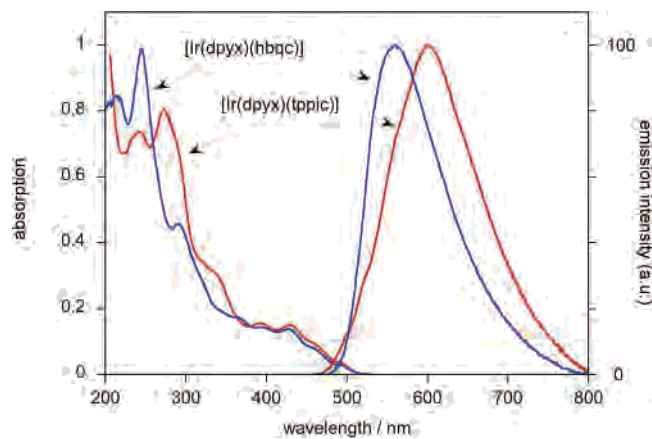


**Figure 7.** Absorption and emission spectra of  $[\text{Ir}(\text{dpyx})(\text{hbqc})]$  (**8**) (blue) and  $[\text{Ir}(\text{dpyx})(\text{tppic})]$  (**7**) (red) in  $\text{CH}_3\text{CN}$  at 295 K;  $\lambda_{\text{ex}} = 460 \text{ nm}$ .

tion ( $\sum k_{\text{nr}} = 1.5 \times 10^5 \text{ s}^{-1}$ ) (Table 3). Gradual photodissociation of  $\text{Cl}^-$  is, however, observed in solution upon prolonged irradiation. Interestingly, Haga and co-workers have also observed very intense emission from a bis-benzimidazole-coordinated iridium complex, containing a combination of ppy and Cl in the remaining coordination sites.<sup>26b</sup>

**4.3.  $[\text{Ir}(\text{N}\wedge\text{C}\wedge\text{N})(\text{C}\wedge\text{N}\wedge\text{O})]$  Complexes:  $[\text{Ir}(\text{dpyx})(\text{tppic})]$  (**7**) and  $[\text{Ir}(\text{dpyx})(\text{hbqc})]$  (**8**).** The ground-state absorption spectra of **7** and **8** (Figure 7) show similar features to that of **5**. Again, the bands stretching into the visible region (400–500 nm) are attributed to charge-transfer transitions, blue-shifted with respect to **3**, owing to the weaker ligand field offered by the coordinating oxygen compared to the cyclometalating carbon and consequent reduction in the HOMO energy. In this respect, at least, the  $\text{C}\wedge\text{N}\wedge\text{O}$  ligand is thus apparently similar to the combination of ppy and Cl in **5**.

Both of the  $\text{C}\wedge\text{N}\wedge\text{O}$  complexes show a broad structureless emission band, typical of phosphorescence from  $^3\text{MLCT}$  states. However, DFT calculations suggest that there is a significant amount of dpyx  $\rightarrow$  tppic and dpyx  $\rightarrow$  hbqc LLCT, and LC character in both cases (Figure 8). The emission of **8** ( $\lambda_{\text{max}} = 562 \text{ nm}$ ) is blue-shifted with respect to **3** (585 nm), again attributable to a lower energy HOMO as a result of the replacement of a cyclometalated carbon by the oxygen atom. In contrast, the emission from **7** is significantly red-shifted ( $\lambda_{\text{max}} = 603 \text{ nm}$ ), even though the absorption spectra of both of the  $[\text{Ir}(\text{N}\wedge\text{C}\wedge\text{N})(\text{C}\wedge\text{N}\wedge\text{O})]$  complexes are very similar to one another. This apparent anomaly is probably related to the introduction of the *p*-tolyl substituent. Whereas the HOMO–LUMO gap is likely to be similar in the ground state of the two complexes, an additional stabilization will be possible in the relaxed excited state of the tppic complex by rotation of the *p*-tolyl group into the coplanar conformation required for maximal conjugation. We have observed a similar effect of pendent aryl groups lowering the  $\pi$ – $\pi^*$  emission energy, without significantly affecting the corresponding absorption band, in aryl-substituted  $\text{N}\wedge\text{C}\wedge\text{N}$ -coordinated platinum(II) complexes.<sup>33b</sup>

The luminescence quantum yields of the  $\text{C}\wedge\text{N}\wedge\text{O}$  complexes are substantially lower than for the other complexes described so far, and their lifetimes are very short (Table

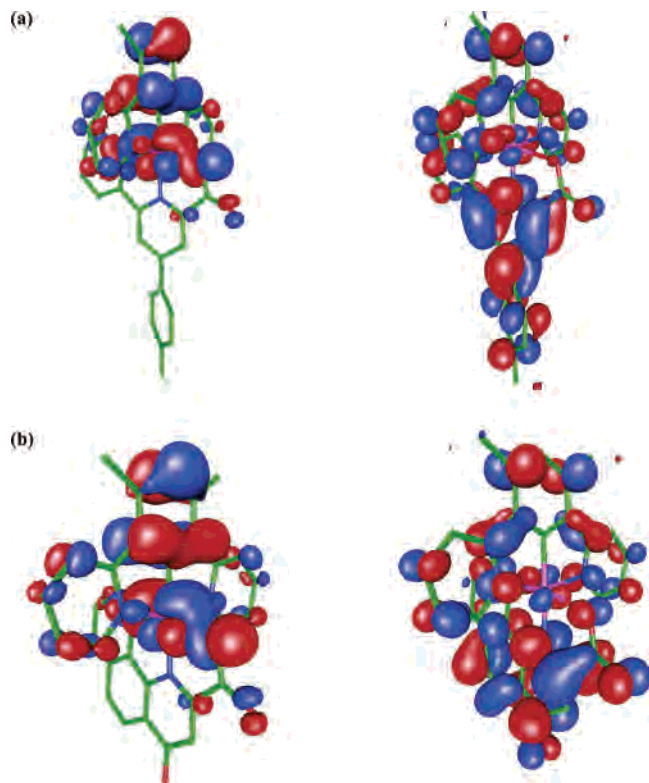


**Figure 8.** DFT calculation of the HOMO (left) and LUMO (right) for [Ir(dpyx)(tppic)] (7) (a) and [Ir(dpyx)(hbqc)] (8) (b).

3). Calculation of the radiative and nonradiative decay rate constants reveals that the poor efficiency of emission is due to rapid nonradiative processes:  $\sum k_{nr}$  is 1–2 orders of magnitude larger than for the [Ir(N $\wedge$ C $\wedge$ N)(C $\wedge$ N $\wedge$ C)] complexes (Table 3). Although we do not have conclusive evidence, we suspect that the large nonradiative decay rate constant is due to a photochemical cleavage of the Ir–O bond in the excited state, analogous to that of the Ir–C bond of **3**. The Ir–O bond would be expected to be labilized by the strong trans influence of the trans-disposed cyclometalated carbon. Whereas photodissociation is irreversible for [Ir(N $\wedge$ C $\wedge$ N)(C $\wedge$ N $\wedge$ C)], however, no net decomposition is observed for the two C $\wedge$ N $\wedge$ O complexes, even upon intense irradiation. Apparently, therefore, the Ir–O bond dissociation is reversible, re-formation of this coordinate bond being possible after nonradiative relaxation to the ground state, to regenerate the starting complex.

**4.4. [Ir(N $\wedge$ C $\wedge$ N)(N $\wedge$ N $\wedge$ N)]<sup>2+</sup> Complexes: [Ir(dpyx)(tpy)]<sup>2+</sup> (**2a**) and [Ir(dpyx)(tppy)]<sup>2+</sup> (**2b**).** These complexes are pale yellow in color, in contrast to the strong orange colors of the other complexes discussed so far. The origin of this difference is clear from the absorption data, which reveal that the bands extending into the visible beyond 400 nm are very weak (Figure 9 and Table 2). These low-energy bands are identified as almost purely dpyx  $\rightarrow$  tpy LLCT transitions on the basis of DFT calculations (Figure 10).

The complexes are scarcely emissive at room temperature:  $\phi < 10^{-3}$  in degassed CH<sub>3</sub>CN. Even at 77 K, **2a** is only very weakly emissive, exhibiting a structured profile with a maximum at 502 nm (Figure 9). The emission is attributed to the dpyx  $\rightarrow$  tpy LLCT transition. Given the

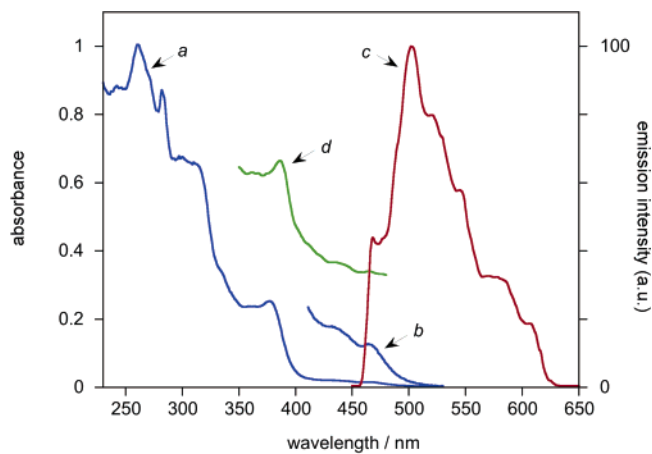


**Figure 9.** Absorption spectrum of [Ir(dpyx)(tpy)](PF<sub>6</sub>)<sub>2</sub> (**2a**) in CH<sub>3</sub>CN at 295 K (blue line, a), with the weak low-energy bands in the 400–500 nm region expanded for clarity (b). The emission spectrum ( $\lambda_{ex} = 370$  nm, red line, c) and low energy portion of the excitation spectrum ( $\lambda_{em} = 501$  nm, green line, d) displayed by this complex in an ethanol/methanol glass (4:1 by volume) at 77 K are also shown.

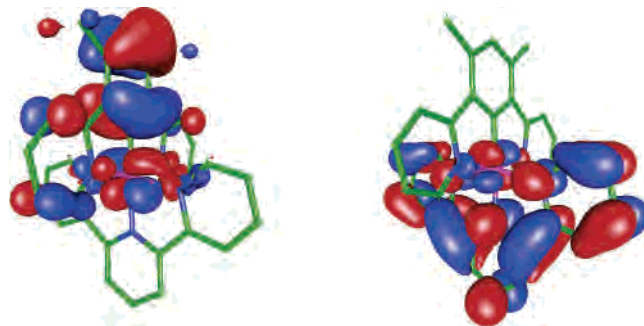


**Figure 10.** DFT calculation of the HOMO (left) and LUMO (right) for [Ir(dpyx)(tpy)]<sup>2+</sup> (**2a**).

small contribution of metal character to the excited state, the oscillator strength and hence radiative rate constant,  $k_r$ , are expected to be particularly small.

Complexes of iridium(III) with an N<sub>3</sub>C donor set are rare. Of the three instances in the literature, although no quantum yield has been reported for the complex [Ir(bpy)<sub>2</sub>(ppy)]<sup>2+</sup>,<sup>6b,47</sup> there was no suggestion that emission was particularly weak,<sup>6b</sup> while [Ir(bpy-*N,N'*)<sub>2</sub>(Hbpy-C<sup>3</sup>,*N'*)]<sup>2+</sup> was reported to have a high quantum yield of 0.30.<sup>48</sup> It is likely that in these tris-bidentate complexes, there is greater MLCT character, promoting the radiative transition. In contrast, the bis-terdentate, mono-cyclometalated complex [Ir(bmpqpyH-N $\wedge$ N $\wedge$ N)(bmpqpy-N $\wedge$ N $\wedge$ C)]<sup>2+</sup> exhibits a luminescence quantum yield of only 0.005 in deoxygenated acetonitrile solution,<sup>23</sup> behavior more consistent with that observed here for [Ir(dpyx)(tpy)]<sup>2+</sup> {bmpqpyH = 2,6-bis(7'-methyl-4'-phenyl-2'-quinolyl)-pyridine}.

Given the poor emission properties of this class of complex, the strategy for obtaining emissive, charge-neutral complexes represented by Class IV in Scheme 1 is clearly not a viable one.

(47) Constable, E. C.; Leese, T. A. *J. Organomet. Chem.* **1987**, 335, 293.

(48) (a) Watts, R. J.; Harrington, J. S.; van Houton, J. *J. Am. Chem. Soc.* **1977**, 99, 2179. (b) Braterman, P. S.; Heath, G. A.; MacKenzie, A. J.; Noble, B. C.; Peacock, R. D.; Yellowlees, L. *J. Inorg. Chem.* **1984**, 23, 3425.



## Conclusions

This study demonstrates that a family of iridium(III) complexes that incorporate an N $\wedge$ C $\wedge$ N-coordinating 1,3-di-(2-pyridyl)benzene derivative are accessible. The introduction of methyl substituents at C<sup>4</sup> and C<sup>6</sup> of the phenyl ring blocks competitive cyclometalation at these positions—and hence the alternative bidentate binding mode—greatly facilitating the chemistry in terms of yields and purification. By proceeding via the intermediacy of the dichlorobridged dimer, **1**, complexes with overall charge neutrality can then be obtained through the introduction of a second terdentate ligand, C $\wedge$ N $\wedge$ C or C $\wedge$ N $\wedge$ O-coordinating, or through a combination of a bidentate C $\wedge$ N ligand with a monodentate chloride anion in the sixth site.

The [Ir(N $\wedge$ C $\wedge$ N)(C $\wedge$ N $\wedge$ C)] complexes are strongly emissive in fluid solution at room temperature, from states of predominant MLCT character. For example, the quantum yield of **4** in deoxygenated acetonitrile is comparable to that of the widely studied electrophosphorescent material *fac*-[Ir(ppy)<sub>3</sub>] ( $\phi = 0.44^3$ ), with a similar emission wavelength maximum, while **5** has an exceptionally high quantum yield of 0.76 under the same conditions.

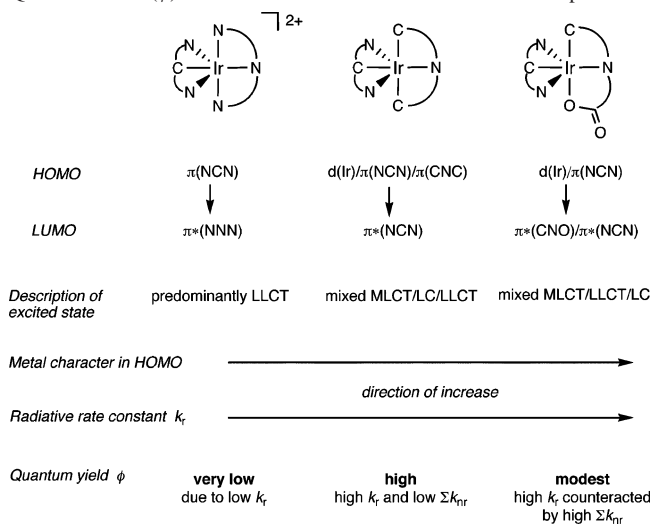
All of the complexes feature a meridional arrangement of the nitrogen atoms. In the case of the [Ir(N $\wedge$ C $\wedge$ N)(C $\wedge$ N $\wedge$ C)] complexes (**3** and **4**), this leads to two mutually *trans*-related Ir–C bonds. Although the complexes show some tendency to photodissociation in solution through cleavage of one of these bonds, owing to the high *trans* influence of C<sup>–</sup>, they are much more stable than *mer*-[Ir(ppy)<sub>3</sub>], as clearly evident from the much smaller nonradiative decay rate constants {e.g.,  $\Sigma k_{nr} = 1.6 \times 10^5 \text{ s}^{-1}$  for [Ir(dpyx)(F<sub>4</sub>dppy)] compared to  $6.5 \times 10^6 \text{ s}^{-1}$  for *mer*-Ir(ppy)<sub>3</sub>}. The [Ir(N $\wedge$ C $\wedge$ N)(C $\wedge$ N $\wedge$ O)] complexes exhibit comparatively low luminescence quantum yields arising from rapid nonradiative decay, possibly due to facile reversible photodissociation of the Ir–O bond positioned *trans* to an Ir–C bond.

Finally, dicationic complexes of the form [Ir(N $\wedge$ C $\wedge$ N)(N $\wedge$ N $\wedge$ N)]<sup>2+</sup> are also readily accessible from **1** through reaction with a terpyridine ligand. These complexes are only weakly emissive, probably associated with the high degree of LLCT character of the excited state, a feature also observed in [Ir(C $\wedge$ N $\wedge$ C)(N $\wedge$ N $\wedge$ N)]<sup>+</sup> complexes.<sup>22</sup>

The trends in frontier orbital characteristics and their influence on the emission properties (radiative rate constant,  $k_r$ , and quantum yield,  $\phi$ ) are illustrated schematically in Scheme 6. The scheme serves to highlight the profound influence of the ligands that complete the coordination sphere of these iridium complexes containing one N $\wedge$ C $\wedge$ N-bound ligand.

In summary, the compounds reported here represent a new family of iridium complexes, in which emission energies and intensities can be correlated with structural changes with the aid of DFT analysis. Apart from potential applicability to light-emitting device technology, the bis-terdentate binding geometries will render such compounds particularly attractive for incorporation into linear supramolecular multimetallic architectures. The absence of chirality circumvents the

**Scheme 6.** Schematic Summary of the Nature of the Frontier Orbitals and of the Trends in Radiative Rate Constant ( $k_r$ ) and Emission Quantum Yield ( $\phi$ ) for the Three Classes of Bis-terdentate Complexes<sup>a</sup>



<sup>a</sup> The properties of the [Ir(N $\wedge$ C $\wedge$ N)(C $\wedge$ N)Cl] complex are broadly similar to those of the [Ir(N $\wedge$ C $\wedge$ N)(C $\wedge$ N $\wedge$ C)] class.

problems associated with diastereoisomer formation encountered with unresolved tris-bidentate complexes, while the ease with which substituents can be incorporated into the central five positions of the ligands will allow for the construction of linear connections between units.<sup>49</sup>

## Experimental Section

4-Tolyl-6-phenylpicolinic acid (tppicH<sub>2</sub>)<sup>51</sup> and 2,6-di(2-thienyl)pyridine (dthpyH<sub>2</sub>)<sup>50</sup> were prepared according to procedures reported previously. 4-Hydroxybenzo[*h*]quinoline-2-carboxylic acid<sup>51</sup> (hbqcH<sub>2</sub>) was supplied by Avecia Ltd. as the ethyl ester, and hydrolyzed to the acid using 5% NaOH(aq) at reflux. The synthesis and characterization data for **3** and **2b** were reported in the Supporting Information of our previous communication.<sup>25</sup>

**1. Synthesis of Ligands. 1.1. 1,3-Di(2-pyridyl)-4,6-dimethylbenzene (dpyxH). 1.1.1. Step 1: Preparation of 1,3-Dibromo-4,6-dimethylbenzene (dibromo-*m*-xylene).** The method was based on a procedure described in the literature,<sup>29</sup> but the yield was found to be greatly improved by using >2 equiv of bromine rather the ~1:1 ratio used previously. Bromine (43.8 g, 274 mmol) was added over 5 min with stirring to *m*-xylene (13.0 g, 122 mmol), followed by addition of iodine (0.5 g, 1.97 mmol) over a further 30 min. The mixture was then stirred at room temperature for a further 3 h. After this period, NaOH solution (4 M, 100 mL) was added and the reaction mixture was stirred for 15 min. The resulting precipitate was isolated by filtration, dried under vacuum, and recrystallized from ethanol to give the desired product as a white solid (15.7 g, 49%). <sup>1</sup>H NMR (CDCl<sub>3</sub>, 200 MHz)  $\delta$  7.68 (1H, s, H<sup>2</sup>), 7.10 (1H, s, H<sup>5</sup>), 2.31 (6H, s, Me). <sup>13</sup>C{<sup>1</sup>H} NMR (CDCl<sub>3</sub>, 126 MHz)  $\delta$  137.0 (C<sup>9</sup>), 135.0 (CH), 132.7 (CH), 122.1 (C<sup>9</sup>), 22.4 (CH<sub>3</sub>). MS(EI)  $m/z$  = 262/264/266 (M<sup>+</sup>), 183/185 (M<sup>+</sup> – Br), 104 (M<sup>+</sup> – 2Br), 103 (M<sup>+</sup> – Br, HBr).

(49) For a recent example of the incorporation of a bis-terdentate complex into a dimetallic assembly through cross-coupling, see: Arm, K. J.; Williams, J. A. G. *Dalton Trans.* **2006**, 2172.

(50) Constable, E. C.; Henney, R. P. G.; Tocher, D. A. *J. Chem. Soc., Dalton Trans.* **1992**, 2467.

(51) Foster, R. E.; Lipscomb, R. D.; Thompson, T. J.; Hamilton, C. S. *J. Am. Chem. Soc.* **1946**, *68*, 1327.



**1.1.2. Step 2: Formation of 1,3-di(2-pyridyl)-4,6-dimethylbenzene.** A mixture of 2-tri-*n*-butylstannylpyridine (9.32 g, 81% pure by mass by  $^1\text{H}$  NMR assay, 20.5 mmol), 1,5-dibromo-2,4-dimethylbenzene (2.28 g, 8.64 mmol), bis(triphenylphosphine)-palladium(II) chloride (225 mg, 0.32 mmol), and lithium chloride (2.68 g, 63.2 mmol) in dry toluene (50 mL) was degassed by five freeze–pump–thaw cycles then heated under reflux under a nitrogen atmosphere for 24 h. The progress of the reaction was followed by TLC (silica, hexane/diethyl ether, 75:25). After the reaction mixture cooled to room temperature, saturated KF solution (20 mL) was added and the solution stirred for 30 min. The precipitated solid was removed by filtration and washed with water (50 mL).  $\text{NaHCO}_3$  solution (10%, 100 mL) was then added to the combined filtrates, extracted into dichloromethane ( $2 \times 200$  mL), and dried over  $\text{MgSO}_4$ . Removal of solvent under reduced pressure and purification of the residue by column chromatography (silica, hexane/diethyl ether, gradient elution from 100:0 to 10:90) gave the desired product as a pale yellow solid (1.35 g, 61%),  $\text{mp} = 83.8\text{--}85.6$  °C.  $^1\text{H}$  NMR ( $\text{CDCl}_3$ , 500 MHz)  $\delta$  8.67 (2H, d,  $J = 4.9$ ,  $\text{H}^6$ ), 7.72 (2H, td,  $J = 7.6$ , 1.8,  $\text{H}^4$ ), 7.47 (1H, s,  $\text{H}^2$ ), 7.43 (2H, d,  $J = 7.7$ ,  $\text{H}^3$ ), 7.27 (1H, s,  $\text{H}^5$ ), 7.23 (2H, ddd,  $J = 7.5$ , 4.9, 1.2,  $\text{H}^5$ ), 2.40 (6H, s, Me).  $^{13}\text{C}\{^1\text{H}\}$  NMR ( $\text{CDCl}_3$ , 126 MHz)  $\delta$  159.8 ( $\text{C}^9$ ), 149.3 ( $\text{C}^6$ ), 138.2 ( $\text{C}^9$ ), 136.2 ( $\text{C}^4$ ), 135.9 ( $\text{C}^9$ ), 133.4 ( $\text{C}^3$ ), 131.2 ( $\text{C}^6$ ), 124.3 ( $\text{C}^3$ ), 121.6 ( $\text{C}^5$ ), 20.1 ( $\text{CH}_3$ ). MS(EI)  $m/z = 260$  ( $\text{M}^+$ ), 259 ( $\text{M}^+ - \text{H}$ ), 245 ( $\text{M}^+ - \text{Me}$ ), 78 ( $\text{C}_5\text{NH}_4^+$ ). MS-(ES+)  $m/z = 261$  ( $[\text{M} + \text{H}]^+$ ), 283 ( $[\text{M} + \text{Na}]^+$ ). HRMS(ES+)  $m/z = 283.1198$  ( $[\text{M} + \text{Na}]^+$ ); Calcd for  $\text{C}_{18}\text{H}_{16}\text{N}_2\text{Na}$ , 283.1211. Found: C, 80.85; H, 6.29; N, 10.28%.  $\text{C}_{18}\text{H}_{16}\text{N}_2 \cdot 1/2\text{H}_2\text{O}$  requires: C, 80.27; H, 6.36; N, 10.40%.  $R_f = 0.6$  on silica in dichloromethane/ethanol, 90:10.

**1.2. 2,6-Di(2,4-difluorophenyl)pyridine ( $\text{F}_4\text{dppyH}_2$ ).** The conditions employed were similar to those used in our earlier work on the application of the Suzuki reaction to the synthesis of terpyridines.<sup>52</sup> A combination of 2,6-dibromopyridine (820 mg, 3.46 mmol), 2,4-difluorophenylboronic acid (1.87 mg, 11.8 mmol), and potassium carbonate (3.23 g, 23.4 mmol) in a mixture of 1,2-dimethoxyethane (16 mL) and water (400  $\mu\text{L}$ ) was degassed by three freeze–pump–thaw cycles. Addition of tetrakis(triphenylphosphine)palladium(0) (274 mg, 0.24 mmol) was followed by stirring at room temperature under a nitrogen atmosphere for 30 min before heating to 90 °C overnight. The progress of the reaction was followed by TLC (alumina, hexane/ether, 50:50). After the mixture cooled to room temperature, the precipitated solid was removed by filtration and washed with 1,2-dimethoxyethane, followed by removal of solvent from the combined filtrates under reduced pressure. The residue was redissolved in dichloromethane (100 mL) and washed with dilute  $\text{NaHCO}_3$  solution ( $3 \times 100$  mL). The organic layer was dried over  $\text{MgSO}_4$ , and the solvent removed under reduced pressure before purification by column chromatography (silica, hexane/diethyl ether, gradient elution from 100:0 to 98:2) to give the desired product as a white solid (929 mg, 88%),  $\text{mp} = 83.6\text{--}84.4$  °C.  $^1\text{H}$  NMR ( $\text{CDCl}_3$ , 500 MHz)  $\delta$  8.14 (2H, td,  $J = 8.8$ , 6.8,  $\text{H}^6$ ), 7.83 (1H, t,  $J = 7.8$ ,  $\text{H}^4$ ), 7.74 (2H, dd,  $J = 7.5$ , 1.9,  $\text{H}^3$ ), 7.03 (2H, td,  $J = 8.3$ , 2.1,  $\text{H}^5$ ), 6.93 (2H, ddd,  $J = 8.8$ , 6.3, 2.4,  $\text{H}^3$ ).  $^{13}\text{C}\{^1\text{H}\}$  NMR ( $\text{CDCl}_3$ , 126 MHz)  $\delta$  163.2 (dd,  $J = 309.4$ , 11.9,  $\text{C}^2$  or  $\text{C}^4$ ), 161.2 (dd,  $J = 311.9$ , 12.1,  $\text{C}^2$  or  $\text{C}^4$ ), 152.4 (d,  $J = 2.7$ ,  $\text{C}^2$ ), 137.3 (s,  $\text{C}^4$ ), 132.4 (dd,  $J = 9.7$ , 4.5,  $\text{C}^6$ ), 123.7 (dd,  $J = 11.7$ , 3.7,  $\text{C}^1$ ), 122.9 (d,  $J = 10.2$ ,  $\text{C}^3$ ), 112.0 (dd,  $J = 21.1$ , 3.5,  $\text{C}^5$ ), 104.5 (dd,  $J = 26.8$ , 25.5,  $\text{C}^3$ ).  $^{19}\text{F}$  NMR ( $\text{CDCl}_3$ , 470 MHz)  $\delta$  -109.5 (1F, m), -112.8 (1F, m). MS(EI)  $m/z = 303$  ( $\text{M}^+$ ).

Found: C, 66.91; H, 3.01; N, 4.64%.  $\text{C}_{17}\text{H}_9\text{F}_4\text{N}$  requires: C, 67.33; H, 2.99; N, 4.62%.  $R_f = 0.6$  on silica in hexane/diethyl ether, 90:10.

**2. Synthesis of Complexes. 2.1.  $[\text{Ir}(\text{dpyb})(\text{tpty})](\text{PF}_6)_2$ .** A suspension of 1,3-di(2-pyridyl)benzene (dpybH) (201 mg, 0.87 mmol) and iridium trichloride trihydrate (299 mg, 0.85 mmol) in a mixture of 2-ethoxyethanol (15 mL) and water (5 mL) was heated under reflux at 130 °C for 2.5 h. After the mixture cooled to room temperature, the precipitated solid was collected by centrifuge, washed with ethanol ( $2 \times 20$  mL), and dried under vacuum to give an orange solid (342 mg). A suspension of this solid (crude  $[\text{Ir}(\text{dpyb})\text{Cl}(\mu\text{-Cl})_2]$ , see Discussion) (320 mg) and 4'-(*p*-tolyl)-2,2':6',2''-terpyridine (tpty) (160 mg, 0.49 mmol), in ethylene glycol (15 mL), was heated to 196 °C under a nitrogen atmosphere for 1 h. After cooling to room temperature, the reaction mixture was added to water (20 mL) and filtered. Saturated  $\text{KPF}_6$  solution was added, and the resulting red precipitate collected by centrifugation, washed with water ( $3 \times 20$  mL), and dried under vacuum. Purification by column chromatography (alumina, acetonitrile) followed by a second column (silica, acetonitrile/water/saturated  $\text{KNO}_3$  solution, gradient elution from 100:0:0 to 93.8:6.0:0.2) gave the desired product as a red solid (8 mg, 1%). The complex was not isolated in sufficient quantities for reliable elemental analysis data to be obtained, but its identity was confirmed spectroscopically:  $^1\text{H}$  NMR ( $d_6$ -acetone, 500 MHz)  $\delta$  9.43 (2H, s,  $\text{H}^3$  tpty), 9.03 (2H, d,  $J = 8.2$ ,  $\text{H}^3$  tpty), 8.42 (2H, d,  $J = 8.1$ ,  $\text{H}^3$  dpyb), 8.33 (2H, d,  $J = 7.9$ ,  $\text{H}^3$  dpyb), 8.23 (2H, d,  $J = 8.2$ ,  $\text{H}^b$  tpty), 8.20 (2H, td,  $J = 8.0$ , 1.3,  $\text{H}^4$  tpty), 7.98 (2H, td,  $J = 7.9$ , 1.3,  $\text{H}^4$  dpyb), 7.84 (2H, d,  $J = 5.8$ ,  $\text{H}^6$  dpyb), 7.73 (1H, t,  $J = 7.9$ ,  $\text{H}^4$  dpyb), 7.57 (2H, dd,  $J = 5.8$ , 1.2,  $\text{H}^6$  tpty), 7.54 (2H, d,  $J = 8.0$ ,  $\text{H}^a$  tpty), 7.45 (2H, ddd,  $J = 7.8$ , 5.7, 1.2,  $\text{H}^5$  tpty), 7.13 (2H, ddd,  $J = 7.3$ , 5.9, 1.2,  $\text{H}^5$  dpyb), 2.48 (3H, s, Me tpty). MS(ES+)  $m/z = 373.5$  ( $\text{M}^{2+}$ ), 892 ( $\text{M}(\text{PF}_6)^+$ ).

**2.2.  $[\text{Ir}(\text{dpyx})(\text{tpty})](\text{PF}_6)_2$  (2a).** A suspension of **1** (41 mg, 0.039 mmol) and 2,2':6',2''-terpyridine (tpty) (22 mg, 0.094 mmol) in ethylene glycol (5 mL) was heated to 196 °C under a nitrogen atmosphere for 1 h. After cooling to room temperature, the reaction mixture was added to water (10 mL) and filtered. Saturated  $\text{KPF}_6$  solution (20 mL) was added, and the resulting yellow precipitate collected by centrifugation, washed with water ( $3 \times 10$  mL), and dried under vacuum. Purification by column chromatography (silica, acetonitrile/water/saturated  $\text{KNO}_3$  solution, gradient elution from 100:0:0 to 93.0:6.8:0.2) gave the desired product as a yellow solid (44 mg, 58%),  $\text{mp} > 250$  °C.  $^1\text{H}$  NMR ( $d_6$ -acetone, 500 MHz)  $\delta$  9.17 (2H, d,  $J = 8.3$ ,  $\text{H}^3$  tpy), 8.83–8.88 (3H, m,  $\text{H}^4$  tpy,  $\text{H}^3$  tpy), 8.46 (2H, d,  $J = 8.5$ ,  $\text{H}^3$  dpyx), 8.22 (2H, td,  $J = 8.0$ , 1.4,  $\text{H}^4$  tpy), 7.98 (2H, ddd,  $J = 8.2$ , 7.6, 1.6,  $\text{H}^4$  dpyx), 7.78 (2H, dd,  $J = 5.8$ , 0.9,  $\text{H}^6$  dpyx), 7.70 (2H, dd,  $J = 5.8$ , 0.8,  $\text{H}^6$  tpy), 7.50 (2H, ddd,  $J = 7.6$ , 5.7, 1.2,  $\text{H}^5$  tpy), 7.43 (1H, s,  $\text{H}^4$  dpyx), 7.11 (2H, ddd,  $J = 7.3$ , 5.8, 1.1,  $\text{H}^5$  dpyx), 3.02 (6H, s, Me).  $^{13}\text{C}\{^1\text{H}\}$  NMR ( $d_6$ -acetone, 126 MHz)  $\delta$  178.3 ( $\text{C}^9$ ), 170.7 ( $\text{C}^9$ ), 160.4 ( $\text{C}^9$ ), 156.2 ( $\text{C}^6$  tpy), 154.5 ( $\text{C}^9$ ), 152.8 ( $\text{C}^6$  dpyx), 142.7 ( $\text{C}^4$  tpy), 142.1 ( $\text{C}^4$  tpy), 141.4 ( $\text{C}^4$  dpyx), 140.6 ( $\text{C}^9$ ), 138.0 ( $\text{C}^9$ ), 133.9 ( $\text{C}^4$  dpyx), 130.1 ( $\text{C}^5$  tpy), 127.6 ( $\text{C}^3$  tpy), 126.6 ( $\text{C}^3$  tpy), 125.5 ( $\text{C}^3$  dpyx), 124.6 ( $\text{C}^5$  dpyx), 22.6 ( $\text{CH}_3$ ). MS(ES+)  $m/z = 342.5$  ( $\text{M}^{2+}$ ), 830 ( $\text{M}(\text{PF}_6)^+$ ). HRMS(ES+)  $m/z = 830.1460$  ( $\text{M}(\text{PF}_6)^+$ ); calcd for  $^{193}\text{-IrC}_{33}\text{H}_{26}\text{F}_6\text{N}_5\text{P}$ , 830.1459. Found: C, 40.08; H, 2.98; N, 6.82%.  $\text{C}_{33}\text{H}_{26}\text{F}_6\text{IrN}_5\text{P}_2$  requires: C, 40.66; H, 2.69; N, 7.18%. One spot by TLC(silica),  $R_f = 0.4$  in acetonitrile/water/saturated  $\text{KNO}_3$  solution, 90:9:1.

**2.3.  $[\text{Ir}(\text{dpyx})(\text{F}_4\text{dppy})]$  (4).** **1** (41 mg, 0.039 mmol), 2,6-di(2,4-difluorophenyl)pyridine ( $\text{F}_4\text{dppyH}_2$ ) (227 mg, 0.75 mmol) and  $\text{AgOTf}$  (40 mg, 0.16 mmol) were ground together in a porcelain

(52) (a) Aspley, C. J.; Williams, J. A. G. *New J. Chem.* **2001**, 25, 1136.  
(b) Leslie, W.; Wild, K.; Arm, K. J.; Williams, J. A. G. *J. Chem. Soc., Perkin Trans. 2* **2002**, 1669.

mortar. The resulting fine powder was heated to 110 °C and stirred under a nitrogen atmosphere for 24 h. After the mixture cooled to room temperature, the product was extracted into dichloromethane (30 mL), and the remaining solid removed by filtration. Removal of solvent under reduced pressure gave a brown residue. This was purified by column chromatography (silica, hexane/diethyl ether, gradient elution from 100:0 to 95:5; the unreacted excess F<sub>4</sub>dppyH<sub>2</sub> elutes first, and can be recovered) followed by a second column (silica, hexane/diethyl ether, gradient elution from 100:0 to 98:2) to give the desired product as a yellow solid (12 mg, 21%), mp > 250 °C. <sup>1</sup>H NMR (CDCl<sub>3</sub>, 500 MHz) δ 8.16 (2H, d, *J* = 8.2, H<sup>3'</sup> F<sub>4</sub>dppy), 8.07 (2H, d, *J* = 8.3, H<sup>3</sup> dpyx), 7.85 (1H, t, *J* = 8.1, H<sup>4'</sup> F<sub>4</sub>dppy), 7.57 (2H, dd, *J* = 5.7, 1.1, H<sup>6</sup> dpyx), 7.49 (2H, ddd, *J* = 7.5, 6.0, 1.5, H<sup>4</sup> dpyx), 6.97 (1H, s, H<sup>4'</sup> dpyx), 6.63 (2H, ddd, *J* = 5.8, 4.9, 1.0, H<sup>5</sup> dpyx), 6.20 (2H, ddd, *J* = 12.8, 9.1, 2.4, H<sup>3</sup> F<sub>4</sub>dppy), 5.65 (2H, dd, *J* = 7.2, 2.4, H<sup>5</sup> F<sub>4</sub>dppy), 2.94 (6H, s, Me dpyx). <sup>13</sup>C{<sup>1</sup>H} NMR (CDCl<sub>3</sub>, 126 MHz) δ 191.2 (C<sup>9</sup>), 176.1 (C<sup>9</sup>), 168.6 (C<sup>9</sup>), 163.1 (dd, *J* = 259.9, 10.3, CF), 162.2 (dd, *J* = 260.8, 10.3, CF), 161.2 (d, *J* = 7.21, C<sup>9</sup>), 149.8 (CH), 138.4 (CH), 137.0 (C<sup>9</sup>), 134.8 (C<sup>9</sup>), 133.8 (CH<sup>6</sup> dpyx), 131.0 (C<sup>9</sup>), 127.2 (CH<sup>4'</sup> dpyx), 122.6 (CH<sup>3</sup> dpyx), 120.5 (CH), 118.0 (dd, *J* = 13.5, 2.6, CH<sup>5</sup> F<sub>4</sub>dppy), 117.6 (d, *J* = 18.8, CH<sup>3'</sup> F<sub>4</sub>dppy), 97.6 (t, *J* = 26.2, CH<sup>3</sup> F<sub>4</sub>dppy), 23.0 (CH<sub>3</sub>). <sup>19</sup>F NMR (CDCl<sub>3</sub>, 282 MHz) δ -110.77 (2F, q, *J* = 8.8), -111.02 (2F, dd, *J* = 13.4, 9.0). MS(ES<sup>+</sup>) *m/z* = 754 ([M + H]<sup>+</sup>). HRMS(ES<sup>+</sup>) *m/z* = 754.1440 ([M + H]<sup>+</sup>); calcd for <sup>193</sup>IrC<sub>35</sub>H<sub>23</sub>F<sub>4</sub>N<sub>3</sub>, 754.1452. Found: C, 55.45; H, 3.34; N, 5.21%. C<sub>35</sub>H<sub>23</sub>F<sub>4</sub>IrN<sub>3</sub> requires: C, 55.77; H, 3.08; N, 5.57%. *R*<sub>f</sub> = 0.2 on silica in hexane/diethyl ether, 90:10.

**2.4. [Ir(dpyx)(ppy)Cl] (5). 1** (35 mg, 0.033 mmol) and AgOTf (44 mg, 0.17 mmol) in 2-phenylpyridine (ppyH) (250 μL, 1.75 mmol) were heated to 110 °C under a nitrogen atmosphere for 24 h. After the mixture cooled to room temperature, dichloromethane (25 mL) was added and the remaining solid removed by filtration. Washing of the filtrate with HCl (1 M, 3 × 25 mL), drying over MgSO<sub>4</sub>, and removal of solvent under reduced pressure gave a yellow residue. This was purified by column chromatography (silica, dichloromethane/methanol, gradient elution from 100:0 to 99.75:0.25) to give the desired product as a yellow solid (25 mg, 59%), mp > 250 °C. <sup>1</sup>H NMR (CDCl<sub>3</sub>, 500 MHz) δ 10.12 (1H, d, *J* = 5.3, H<sup>6</sup> ppy), 8.07 (1H, d, *J* = 8.0, H<sup>3</sup> ppy), 8.00 (2H, d, *J* = 8.4, H<sup>3</sup> dpyx), 7.96 (1H, td, *J* = 8.0, 1.4, H<sup>4</sup> ppy), 7.65 (2H, d, *J* = 5.6, H<sup>6</sup> dpyx), 7.59 (1H, d, *J* = 7.7, H<sup>6'</sup> ppy), 7.51–7.55 (3H, m, H<sup>4</sup> dpyx, H<sup>5</sup> ppy), 6.88 (1H, s, H<sup>4'</sup> dpyx), 6.75 (2H, ddd, *J* = 7.2, 5.9, 1.0, H<sup>5</sup> dpyx), 6.71 (1H, td, *J* = 7.4, 1.2, H<sup>5'</sup> ppy), 6.54 (1H, td, *J* = 7.5, 1.0, H<sup>4'</sup> ppy), 6.00 (1H, d, *J* = 7.7, H<sup>3'</sup> ppy), 2.83 (6H, s, Me). MS(ES<sup>+</sup>) *m/z* = 606 ([M - Cl]<sup>+</sup>), 638 ([M - Cl + MeOH]<sup>+</sup>). Found: C, 53.98; H, 3.81; N, 6.30%. C<sub>29</sub>H<sub>23</sub>ClIrN<sub>3</sub> requires: C, 54.33; H, 3.62; N, 6.55%.

**2.5. [Ir(dpyx)(dthpyH)](CH<sub>3</sub>CO<sub>2</sub>) (6).** A suspension of **1** (41 mg, 0.039 mmol), 2,6-di(2-thienyl)pyridine (dthpyH<sub>2</sub>) (29 mg, 0.12 mmol), and AgOTf (86 mg, 0.33 mmol) in glacial acetic acid (2 mL) was heated to 110 °C under a nitrogen atmosphere overnight. After the mixture cooled to room temperature, water (20 mL) was added and the mixture extracted into dichloromethane (3 × 20 mL), dried over MgSO<sub>4</sub>, and filtered. Removal of solvent under reduced pressure followed by purification by column chromatography (silica, dichloromethane/methanol, gradient elution from 100:0 to 95:5) gave the product as a yellow solid (10 mg, 36%), mp > 250 °C. Elemental analysis data was inconclusive due to the ambiguity of coordination at the sixth site (L in Scheme 5). <sup>1</sup>H NMR (CDCl<sub>3</sub>, 400 MHz) δ 8.22 (1H, dd, *J* = 7.9, 1.4, H<sup>5'</sup> dthpyH), 8.19 (1H, t, *J* = 7.8, H<sup>4'</sup> dthpyH), 8.07 (2H, d, *J* = 8.5, H<sup>3</sup> dpyx), 7.95 (1H, dd, *J* = 3.8, 0.8, H<sup>5''</sup> dthpyH), 7.75 (2H, ddd, *J* = 8.3, 7.6, 1.7, H<sup>4</sup>

dpyx), 7.70 (1H, dd, *J* = 7.5, 1.4, H<sup>3'</sup> dthpyH), 7.34 (2H, ddd, *J* = 5.8, 1.6, 0.6, H<sup>6</sup> dpyx), 7.17 (1H, dd, *J* = 5.2, 3.8, H<sup>4''</sup> dthpyH), 7.07 (1H, s, H<sup>4'</sup> dpyx), 7.04 (1H, dd, *J* = 5.2, 0.7, H<sup>5''</sup> dthpyH), 7.03 (1H, d, *J* = 4.9, H<sup>5</sup> dthpyH), 6.99 (2H, ddd, *J* = 7.5, 5.7, 1.3, H<sup>5</sup> dpyx), 5.69 (1H, d, *J* = 4.9, H<sup>4</sup> dthpyH), 2.86 (6H, s, CH<sub>3</sub>). <sup>13</sup>C{<sup>1</sup>H} NMR (CDCl<sub>3</sub>, 101 MHz) δ 174.2 (C<sup>9</sup>), 169.6 (C<sup>9</sup>), 159.0 (C<sup>9</sup>), 151.7 (CH), 149.2 (C<sup>9</sup>), 148.7 (C<sup>9</sup>), 140.8 (CH), 139.2 (C<sup>9</sup>), 138.8 (C<sup>4</sup> dpyx), 138.3 (C<sup>9</sup>), 138.0 (C<sup>9</sup>), 135.5 (C<sup>9</sup>), 134.3 (C<sup>4''</sup> dthpyH), 132.9 (C<sup>3''</sup> dthpyH), 131.9 (C<sup>4'</sup> dpyx), 130.2 (C<sup>4</sup> dthpyH), 128.9 (C<sup>5</sup> dthpyH or C<sup>5''</sup> dthpyH), 127.8 (CH), 123.4 (C<sup>3</sup> dpyx), 123.2 (C<sup>5</sup> dpyx), 117.4 (C<sup>3'</sup> dthpyH), 117.1 (CH), 22.7 (CH<sub>3</sub>). MS-(ES<sup>+</sup>) *m/z* = 694 (M<sup>+</sup>). HRMS(ES<sup>+</sup>) *m/z* = 694.0966 (M<sup>+</sup>); calcd for <sup>193</sup>IrC<sub>31</sub>H<sub>23</sub>N<sub>3</sub>S<sub>2</sub>, 694.0963.

**2.6. [Ir(dpyx)(tppic)] (7). 1** (373 mg, 0.36 mmol), 4-*p*-tolyl-6-phenylpicolinic acid (tppicH<sub>2</sub>) (1.03 g, 3.55 mmol), AgOTf (552 mg, 2.15 mmol), and benzoic acid (3.49 g, 28.6 mmol) were ground together in a porcelain mortar. The resulting fine powder was heated to 150 °C and stirred under a nitrogen atmosphere for 24 h. After the mixture cooled to room temperature, the product was dissolved in dichloromethane (50 mL) and washed with sodium hydrogen carbonate solution (1 M, 3 × 50 mL). Drying over Na<sub>2</sub>CO<sub>3</sub> was followed by removal of solvent under reduced pressure. The brown residue was purified by column chromatography (silica, dichloromethane/methanol, gradient elution from 100:0 to 97:3) to give the desired product as an orange solid (286 mg, 54%), mp > 250 °C. <sup>1</sup>H NMR (CDCl<sub>3</sub>, 500 MHz) δ 8.48 (1H, d, *J* = 1.3, H<sup>3</sup> tpic), 8.31 (1H, d, *J* = 1.4, H<sup>5</sup> tpic), 8.04 (2H, d, *J* = 8.1, H<sup>6</sup> dpyx), 7.86 (2H, d, *J* = 8.1, H<sup>b</sup> tpic), 7.70 (1H, dd, *J* = 7.9, 1.3, H<sup>6'</sup> tpic), 7.59 (2H, ddd, *J* = 8.1, 7.7, 1.5, H<sup>5</sup> dpyx), 7.41–7.44 (4H, m, H<sup>a</sup> tpic, H<sup>3</sup> dpyx), 6.94 (1H, s, H<sup>4'</sup> dpyx), 6.79 (2H, ddd, *J* = 7.1, 6.0, 1.0, H<sup>4</sup> dpyx), 6.78 (1H, ddd, *J* = 8.7, 7.7, 1.3, H<sup>5'</sup> tpic), 6.57 (1H, td, *J* = 7.5, 1.2, H<sup>4'</sup> tpic), 5.82 (1H, dd, *J* = 7.8, 1.0, H<sup>3'</sup> tpic), 2.86 (6H, s, Me dpyx), 2.51 (3H, s, Me tpic). MS-(ES<sup>+</sup>) *m/z* = 740 ([M + H]<sup>+</sup>). MS(EI) *m/z* = 739 (M<sup>+</sup>, 695 (M<sup>+</sup> - CO<sub>2</sub>), 347.5 (M<sup>2+</sup> - CO<sub>2</sub>). HRMS(ES<sup>+</sup>) *m/z* = 740.1881 ([M + H]<sup>+</sup>); calcd for <sup>193</sup>IrC<sub>37</sub>H<sub>29</sub>O<sub>2</sub>N<sub>3</sub>, 740.1884. Found: C, 59.74; H, 4.28; N, 5.52%. C<sub>37</sub>H<sub>29</sub>IrN<sub>3</sub>O<sub>2</sub> requires: C, 60.07; H, 3.95; N, 5.68%. *R*<sub>f</sub> = 0.5 in dichloromethane/methanol, 90:10.

**2.7. [Ir(dpyx)(hbqc)] (8). 1** (40 mg, 0.038 mmol), 4-hydroxybenzo[*h*]quinoline-2-carboxylic acid (hbqcH<sub>2</sub>) (87 mg, 0.36 mmol), AgOTf (59 mg, 0.23 mmol), and benzoic acid (314 mg, 2.57 mmol) were ground together in an agar mortar. The resulting fine powder was heated to 110 °C and stirred under a nitrogen atmosphere for 24 h. After the mixture cooled to room temperature, the solid was extracted into acetonitrile and filtered through Celite, followed by removal of solvent under reduced pressure. The residue was dissolved in the minimum amount of acetonitrile and added to water (50 mL). The resulting yellow precipitate was collected by centrifugation, washed with water (3 × 10 mL), and dried under vacuum. The solid, which may be solubilized in dichloromethane by the addition of a few drops of trifluoroacetic acid, was purified by column chromatography (silica, dichloromethane/methanol, gradient elution from 100:0 to 97.5:2.5) to give the desired product as a yellow solid (30 mg, 58%), mp > 250 °C. <sup>1</sup>H NMR (CDCl<sub>3</sub>, 500 MHz) δ 8.12 (1H, d, *J* = 9.0, H<sup>5</sup> hbqc), 8.12 (1H, s, H<sup>3</sup> hbqc), 8.06 (2H, d, *J* = 8.4, H<sup>3</sup> dpyx), 7.83 (1H, d, *J* = 9.0, H<sup>6</sup> hbqc), 7.63 (2H, td, *J* = 7.9, 1.7, H<sup>4</sup> dpyx), 7.28 (2H, d, *J* = 5.8, H<sup>6</sup> dpyx), 7.25 (1H, d, *J* = 7.4, H<sup>7</sup> hbqc), 7.00 (1H, br s, H<sup>4'</sup> dpyx), 6.90 (1H, t, *J* = 7.6, H<sup>8</sup> hbqc), 6.78 (2H, ddd, *J* = 7.0, 5.8, 1.0, H<sup>5</sup> dpyx), 5.86 (1H, d, *J* = 7.5, H<sup>9</sup> hbqc), 2.87 (6H, s, Me dpyx). <sup>13</sup>C{<sup>1</sup>H} NMR (CDCl<sub>3</sub>, 126 MHz) δ 183.8, 175.3, 171.0, 163.3, 151.5, 151.0, 144.5, 140.8, 138.1 (C<sup>4</sup> dpyx), 138.1, 137.8, 134.8, 133.3, 130.7 (C<sup>6</sup> hbqc), 130.4, 129.4 (C<sup>8</sup> hbqc), 123.0 (C<sup>3</sup> dpyx),

122.2 (C<sup>5</sup> dpyx), 120.9, 120.2, 119.5, 118.9, 108.1 (C<sup>5</sup> hbqc or C<sup>3</sup> hbqc), 22.6 (CH<sub>3</sub> dpyx). MS(ES<sup>+</sup>)  $m/z$  = 690 ([M + H]<sup>+</sup>). HRMS-(ES<sup>+</sup>)  $m/z$  = 690.1364 ([M + H]<sup>+</sup>); calcd for <sup>193</sup>IrC<sub>32</sub>H<sub>23</sub>O<sub>3</sub>N<sub>3</sub>, 690.1363.  $R_f$  = 0.3 in dichloromethane/methanol, 90:10. Found: C, 55.26; H, 3.40; N, 5.74%. C<sub>32</sub>H<sub>22</sub>IrN<sub>3</sub>O<sub>3</sub> requires: C, 55.80; H, 3.22.; N, 6.10%.

**3. Photophysical Measurements.** Absorption spectra were measured on a Biotek Instruments XS spectrometer, using quartz cuvettes of 1 cm path length. Steady-state luminescence spectra were measured using a Jobin Yvon FluoroMax-2 spectrofluorimeter, fitted with a red-sensitive Hamamatsu R928 photomultiplier tube; the spectra shown are corrected for the wavelength dependence of the detector, and the quoted emission maxima refer to the values after correction. Samples for emission measurements were contained within quartz cuvettes of 1 cm path length modified with appropriate glassware to allow connection to a high-vacuum line. Degassing was achieved via a minimum of three freeze-pump-thaw cycles while connected to the vacuum manifold; final vapor pressure at 77 K was <10<sup>-2</sup> mbar, as monitored using a Pirani gauge. Luminescence quantum yields were determined by the method of continuous dilution, using [Ru(bpy)<sub>3</sub>]Cl<sub>2</sub> in air-equilibrated aqueous solution ( $\phi$  = 0.028<sup>53</sup>) as the standard; estimated uncertainty in  $\phi$  is  $\pm 20\%$  or better.

Samples for time-resolved measurements were excited at 355 nm using the third harmonic of a Q-switched Nd:YAG laser. The luminescence was detected with a Hamamatsu R928 photomultiplier tube and recorded using a digital storage oscilloscope, before transfer to a PC for analysis. The estimated uncertainty in the quoted lifetimes is  $\pm 10\%$  or better. Bimolecular rate constants for quenching by molecular oxygen,  $k_Q$ , were determined from the lifetimes in degassed and air-equilibrated solution, taking the concentration of oxygen in CH<sub>3</sub>CN at 0.21 atm O<sub>2</sub> to be 1.9 mmol dm<sup>-3</sup>.<sup>54</sup> Where lifetimes in aerated solution were too short to be measured accurately using the available instrumentation,  $k_Q$  was estimated from the corresponding integrated emission intensities.

**4. Crystallography.** The single-crystal X-ray diffraction experiment was carried out at 120 K, using graphite-monochromated Mo

K $\alpha$  radiation ( $\lambda$  = 0.71073 Å) on a Bruker SMART 1K area detector diffractometer, equipped with a Oxford Cryosystems N<sub>2</sub> open-flow cooling device. Series of narrow  $\omega$  scans (0.3°) were performed at several  $\varphi$  settings in such a way as to cover a sphere of data to a maximum resolution between 0.70 and 0.77 Å. Cell parameters were determined and refined using the Bruker SMART software,<sup>55</sup> and raw frame data were integrated using the Bruker SAINT program.<sup>56</sup> The structure was solved by direct methods and refined by full-matrix least squares on  $F^2$  using SHELX.<sup>57</sup> Reflection intensities were corrected by numerical integration using SADABS.<sup>58</sup> All non-hydrogen atoms were refined with anisotropic displacement parameters, and the hydrogen atoms were positioned geometrically and refined using a riding model. Crystal data and structure refinement parameters: C<sub>20</sub>H<sub>21</sub>Cl<sub>2</sub>IrN<sub>2</sub>OS;  $M_r$  = 600.55;  $T$  = 120(2) K;  $\lambda$ (Mo K $\alpha$ ) = 0.71073 Å; monoclinic, space group  $P2_1/n$   $a$  = 14.379(11) Å,  $b$  = 8.779(7) Å,  $c$  = 15.889(12) Å,  $\beta$  = 97.811(7)°,  $V$  = 1987(3) Å<sup>3</sup>;  $D_c$  = 2.007 Mg m<sup>-3</sup>;  $Z$  = 4;  $\mu$ (Mo K $\alpha$ ) = 7.107 mm<sup>-1</sup>; reflections collected/unique 21 215/4559 [ $R_{int}$  = 0.0296]; final  $R$  indices [ $I > 2\sigma(I)$ ]:  $R1$  = 0.0191 and  $wR2$  = 0.0487 [6262];  $R$  indices (all data):  $R1$  = 0.0237 and  $wR2$  = 0.0496.

**Acknowledgment.** We thank the EPSRC and Avecia Ltd for a CASE studentship (to A.J.W.), Frontier Scientific Ltd for key starting materials, the EPSRC National Mass Spectrometry Service Centre for several mass spectra, and Dr. A. Beeby for access to the laser system.

**Supporting Information Available:** Crystallographic data in CIF format; results of structural calculations. This material is available free of charge via the Internet at <http://pubs.acs.org>.

IC061172L

(53) Nakamaru, K. *Bull. Chem. Soc. Jpn.* **1982**, *55*, 2697.

(54) Murov, S. L.; Carmichael, I.; Hug, G. L. *Handbook of Photochemistry*, 2nd ed.; Marcel Dekker: New York, 1993.

(55) SMART, *Data Collection Software*, version 5.625; Bruker Analytical X-ray Instruments Inc.: Madison, WI, 2001.

(56) SAINT, *Data Reduction Software*, version 6.02A.; Bruker Analytical X-ray Instruments Inc.: Madison, WI, 2001.

(57) Sheldrick, G. M. SHELX. *Acta Crystallogr.* **1990**, *A46*, 467–473.

(58) Sheldrick, G. M. SADABS, Version 2.03; University of Göttingen: Göttingen, Germany, 2002.